



Implementation of Walking Pattern Generator and Stability Analysis for Biped Robot Walking on Deformable Surface

by

David T. Butterworth

*Submitted to the
School of Information Technology and Electrical Engineering
in partial fulfillment of the requirements for the degree of*

*Bachelor of Engineering (Honors)
in the division of Mechatronic Engineering (Extended Major)*

at the

*University of Queensland
November 2013*

Thesis Supervisor:

Dr Surya P. N. Singh

Senior Lecturer and Mechatronics Plan Director, School of ITEE, UQ

Thesis Examiner:

Dr Hanna Kurniawati

Lecturer, School of ITEE, UQ

Acknowledgments

The HUBO series humanoid robot platform was developed by Prof Jun-Ho Oh at the Humanoid Robot Research Center at KAIST (Korea Institute of Advanced Science & Technology) and is manufactured by Rainbow Inc. Thank you to Dr Jungho Lee from Rainbow Co. for his expert knowledge of HUBO software.

Thank you to Dr Olivier Stasse from LAAS-CNRS for his assistance with the JRL humanoid dynamics software.

Thanks to Boon Siew Han from the A*STAR Social Robotics Lab for inviting me to work at the lab, and Albertus Hendrawan Adiwahono and Tai Wen Chang for assisting me with experiments.

Dr Surya Singh has been an excellent advisor and mentor. Our many conversations have always been interesting and insightful, and I am grateful for all your help. Thank you for supporting me.

Abstract

Previous research has demonstrated that position-controlled biped robots can walk on rigid surfaces that are flat, lightly sloped or of uneven height. Typically the robot is assumed to be a perfectly rigid kinematic chain and that foot contact is parallel to the floor for ZMP walking methods. It is possible to compensate for a small amount of compliance using feedback control and indeed having some compliance in the ankle and foot can help to damp out vibration. However, too much ankle compliance makes the rigid-body biped uncontrollable and too much deformation in the floor destabilizes the walking gait. This thesis shows that when the robot walks on a deformable surface the destabilizing effect is comparable to the effect of the robot being pushed, which both induce a tipping moment around the edge of the foot. Because the robot is rigid with a floating base, both cases show lateral and/or fore-aft oscillations about the foot, the difference being that the deformable floor induces some twist on the landing foot. This leads to the useful conclusion that existing methods for push recovery on rigid surfaces may be applicable to walking on a deformable floor, however because parallel foot contact can not be assumed then additional controllers must be developed to ensure the foot remains in contact with the non-rigid floor.

Contents

Acknowledgments	i
Abstract	ii
List of Figures	vii
List of Tables	viii
1 Introduction	1
1.1 Aim of Thesis	2
1.2 Contribution	2
2 Background	4
2.1 Humanoid Robots	4
2.2 Walking Robots	5
2.3 Deformable Surfaces	7
2.4 Project Background	9
3 Methods for Robot Walking	11
3.1 Parametrized Cubic Polynomials	13
3.2 ZMP Preview Control	17
3.3 Model Predictive Control	20
4 Simulation Environment	22
4.1 Physics Simulators	22

4.2	Robot Model	24
4.3	World Model	26
4.4	Model Validation	27
5	Robot Controller	29
6	Walking Stability	31
7	Experiments	34
7.1	Testing the new WPG	34
7.2	A Compliant Floor	34
7.3	Impulse Disturbance	34
8	Results and Discussion	36
8.1	New Walking Pattern Generator	36
8.2	Testing on the Real Robot	38
8.3	Deformable Floor and a Push	38
8.4	Conclusions	42

List of Figures

1.1	Currently biped robots must be operated with fall-arrest protection. Two open problems are ensuring biped stability in unknown environments and safety around humans.	3
1.2	Rigid-body model of a humanoid robot subjected to a push. A general approach is to adjust the landing position of the swing foot, however if the robot is pushed towards the support foot in a lateral direction (fig. left) or backwards while walking (fig. right) the problem is more difficult.	3
2.1	Vision for the future: A general-purpose humanoid for elder care, the RI-MAN has soft compliant “skin”. (RIKEN Lab Japan)	5
2.2	Evolution of the NASA-JSC-UTexas Biped (aka Robonaut), an entrant in the DRC (DARPA Robotics Challenge).	7
2.3	Walking test with the HUBO2 robot	10
3.1	Coordinate frames for polynomial walking pattern: forward (sagittal plane) and sway (coronal plane)	14
3.2	WPG using 2-stage ZMP Preview	17
4.1	Simulation model of the HUBO2 robot	25
4.2	Simulated HUBO2 robot walking around obstacles	27
4.3	The compliant joint in the ankle of the real robot is modeled with a sprung ball joint	28

5.1	Embedded PC removed from robot, for testing the control software . . .	29
5.2	HUBO2 visualization in ROS receives joint commands from Control PC	30
6.1	Stability metrics for a humanoid robot	31
6.2	Left: Statically stable, GCOM is inside the SP. Right: Dynamically stable, the GCOM is outside the SP, but the ZMP is inside the SP. . .	32
6.3	Evolution through time of COM, ZMP COP in the $x - y$ plane . . .	33
6.4	Fore-aft stability margin, x distance between ZMP and SP	33
6.5	Lateral stability margin, y distance between ZMP and SP	33
7.1	Left: Robot makes one step on compliant surface. Right: Robot is pushed while mid-step.	35
8.1	Footstep path & evolution of COP whilst walking around obstacle, using Polynomial WPG in simulation	37
8.2	Footstep path & evolution of COP whilst walking around obstacle, using ZMP Preview WPG in simulation	37
8.3	Footstep path & evolution of COP whilst walking around obstacle, using MPC WPG in simulation	37
8.4	Robot makes one step on compliant surface, footstep path & evolution of COP in simulation	39
8.5	Robot is pushed while mid-step, footstep path & evolution of COP in simulation	39
8.6	Lateral stability margin (y ZMP) while walking on rigid floor	40
8.7	Lateral stability margin (y ZMP) with deformable floor segment . . .	40
8.8	Lateral stability margin (y ZMP) with a push	40
8.9	Lateral stability (y axis) for floor segment with increasing deformation (SoftCFM) in simulation	41

- 8.10 When the rigid biped is pushed, a tipping moment acts on the edge of the foot making the robot underactuated (left). A highly deformable floor will also destabilize the robot and induce a similar tipping moment. 41

List of Tables

3.1	Parameters for Polynomial WPG	14
4.1	Physics Engines	23
4.2	Robot Simulation Software	23
4.3	Comparison of downward force acting on each ankle in static position	28

Chapter 1

Introduction

Human-like robots having two arms and two legs will be useful for applications involving tools or environments that were designed for humans, such as caring for the elderly in a cluttered two storey house, or preventing an industrial disaster by opening safety valves. Previous research has demonstrated that humanoid robots can walk on rigid surfaces like a flat floor, a sloping floor, or surfaces with varying heights such as steps or stairs. Typically this requires specific control software for each scenario and if there is some unexpected variation in the floor surface the robot can easily fall. Therefore, usually a human must supervise the robot by operating a fall protection harness (Fig. 1.1) as the robot walks.

To date, there has been little research related to bipeds walking on deformable surfaces, like spongy carpet or sand, and so this thesis analyzes the stability of a rigid position-controlled humanoid walking on a non-rigid office floor comprising of timber and carpet. One might imagine that walking on a carpeted floor is softer and therefore easier than a hard rigid surface, however when there is significant deformation this has a destabilizing effect.

Chap. 2 will consider the extreme example of walking on a trampoline, to illustrate how surfaces can both absorb and reconstitute energy, and that the direction of the ground reaction force on the robot's foot can be unpredictable when a complex deformation model is not available. The contribution of this thesis is to show that

when a position-controlled biped robot is walking on a deformable floor, the effect of the disturbance is comparable to the effect of someone repeatedly pushing the robot while operating on a rigid floor, which suggests we can extend existing methods of ‘push-recovery’ (Fig. 1.2) that assume a rigid floor.

1.1 Aim of Thesis

The aim of this research project was to implement a new Walking Pattern Generator for the full-sized Humanoid Robot HUBO2, and analyze the walking stability, for walking on a deformable surface like the compliant wood-and-carpet floor typically found in an office building.

1.2 Contribution

The contributions of this work are:

- A more realistic dynamic simulation model of the HUBO2 robot
- To describe how methods for biped walking that are typically demonstrated in simulation do not directly scale-up to a full-sized humanoid robot
- To show how the effect of a disturbance caused by the floor surface deforming under the robot’s foot is comparable to the effect of the robot being pushed, indicating that ‘push recovery’ methods might be applicable for walking on these types of surfaces

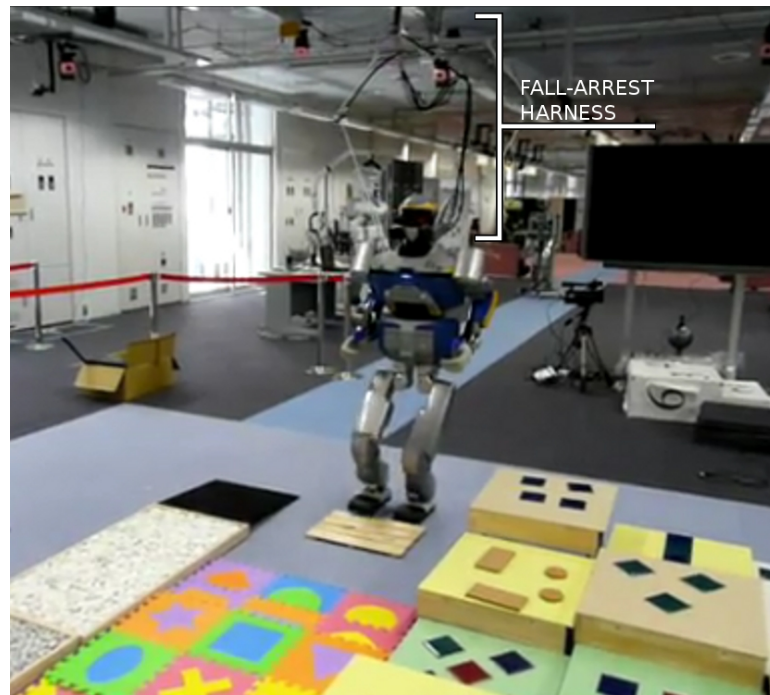


Figure 1.1: Currently biped robots must be operated with fall-arrest protection. Two open problems are ensuring biped stability in unknown environments and safety around humans.

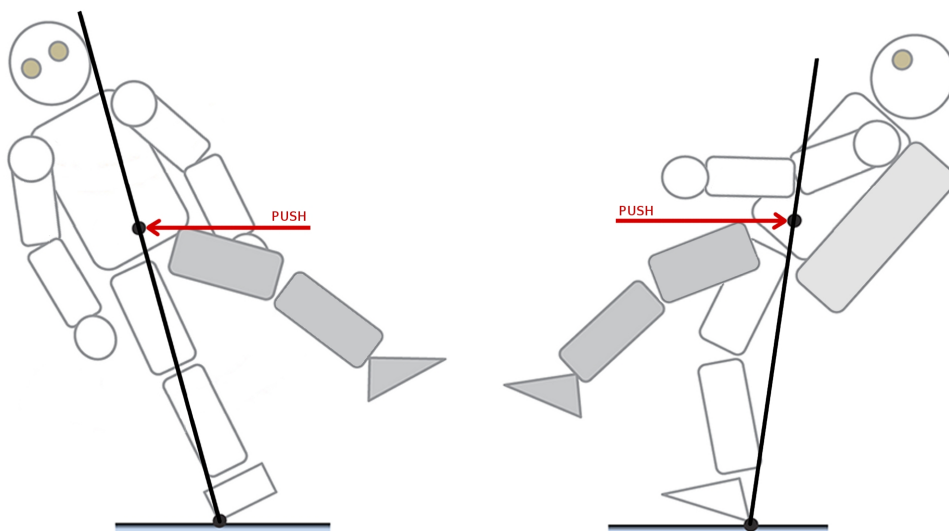


Figure 1.2: Rigid-body model of a humanoid robot subjected to a push. A general approach is to adjust the landing position of the swing foot, however if the robot is pushed towards the support foot in a lateral direction (fig. left) or backwards while walking (fig. right) the problem is more difficult.

Chapter 2

Background

2.1 Humanoid Robots

Humanoid robots are those which have human-like, or anthropomorphic, features. This category includes mobile robots having wheels and a humanoid torso, but this thesis is specifically concerned with electrically powered, high-impedance position controlled bipedal humanoid robots.

Inspired by science fiction, people have high expectations for such robots, but their main application to date has been for entertainment or promotional purposes. Nevertheless, research into humanoid robots has many useful outcomes:

- Encouraging students to study STEM (Science Technology Engineering Mathematics) related disciplines [1]
- Development of bionic knees and legs, that act as limb replacements or enable power-assisted walking [2][3][4]
- Robot nurses that care for aging people in their own home, with the ability to navigate stairs or cluttered floors [5]
- Limited-autonomy robots that can enter hazardous sites or disaster areas and use available tools designed for humans [6][7]

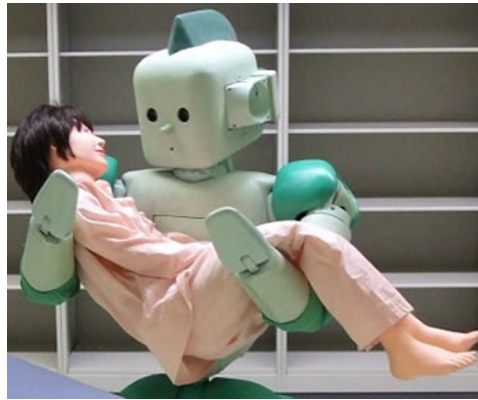


Figure 2.1: Vision for the future: A general-purpose humanoid for elder care, the RI-MAN has soft compliant “skin”. (RIKEN Lab Japan)

2.2 Walking Robots

Numerous bipedal robots and walking machines have been developed. Most position-controlled walking robots use algorithms based on fundamental research into ZMP (Zero Moment Point) dynamics by Vukobratovic [8] and the Honda Motor Company. The following list of ZMP-based, biped humanoid robots highlights that this has been the most successful method to date, and such robots have demonstrated almost every capability that a robot can do whilst operating on a rigid floor with a fall-arrest harness:

- Asimo [9], Honda Research Institute, Japan & United States.
The most famous example, with the smoothest pre-planned walking gait.
- WABOT/WABIAN series’ [10], Waseda University, Japan
- H6 [11], H7 [12], University of Tokyo, Japan
- HRP-2/3/4 series’ [13], Kawada Industries Inc. & AIST (National Institute of Advanced Industrial Science and Technology), Japan
- JOHNNIE [14], Lola [15], TUM (Technical University of Munich), Germany
- Partner [16], Toyota Motor Corp., Japan
- KHR-1/2/3, HUBO [17], HUBO2 series, KAIST, Korea

- REEM-A/B [18], PAL Robotics S.L., Spain
- Mahru-I/II/III/M/R/Z [19], Samsung Electronics Co. Ltd., Korea
- SDR/QRIO[20], Sony Corp., Japan [small sized]
- HOAP-1/2/3 [21], Fujitsu Automation Ltd., Japan [small sized]
- NAO [22], Aldebaran, France [toy sized]
- DARwin-OP [23], sold by Robotis, Korea [toy sized]

This list includes the only two commercially available full-sized humanoid robots REEM-C and HUBO2+. Whilst ZMP-based walking may be considered an old approach, the previous success and availability of equipment meant that implementing ZMP-based algorithms were the best initial approach for looking at walking on deformable surfaces.

In contrast to high-impedance position control is low-impedance force control, which aims to exploit the natural dynamics of the machine towards developing stable locomotion on rough terrain. Fundamental work includes hopping robots by Raibert [24] and the invention of SEA (Series Elastic Actuators) by Pratt [25]. Force controlled biped robots such as the CoMAN [26] have demonstrated improved disturbance rejection and Samsung's RoboRay [27] can walk down a slope with a human-like stretched-leg gait.

Pratt developed an (in)stability criteria called the Capture Point [28] which has been used for push recovery on the M2V2 biped [29]. Recently a Capture Point based framework for walking was implemented on the DLR Biped [30], and the winner of the DARPA VRC (Virtual Robotics Challenge) IHMC (Institute for Human & Machine Cognition) used an ICP (Instantaneous Capture Point) walking controller as part of a larger whole-body control framework.

The important difference is that a position-controlled humanoid is mechanically designed to be perfectly rigid, and is thus modeled as a rigid system. The effect of a



Figure 2.2: Evolution of the NASA-JSC-UTexas Biped (aka Robonaut), an entrant in the DRC (DARPA Robotics Challenge).

disturbance on a rigid biped could be likened to locking one's knees and elbows and attempting to walk across the room, which results in a strange penguin-like gait.

In this thesis a complete multi-link model of the robot is used as part of the Walking Pattern Generator, but with the dynamics simplified to only the linear and angular velocity of each link. Experiments on the real robot suggest that this is not advantageous when there is significant unmodeled compliance, and in fact other work utilizing a simple reaction wheel inverted pendulum suggests that the linear and angular momentum of the COM (Center of Mass) is more fundamental to balance control.

2.3 Deformable Surfaces

From a dynamics perspective, a deformable surface may simply absorb energy (sand, mud) or both store and retribute energy (timber, carpet underlay, trampoline, mattress, chair). This thesis focuses on an office-like floor that primarily deforms and absorbs energy, with minimal restitution. It is interesting to notice that these two categories also differentiate humanoids that might operate on outdoor versus indoor

terrain.

The idea of balancing on a pillow may seem strange, but this physiotherapy exercise [31] would be a good benchmark for an agile humanoid. In biomechanics, McMahon’s work [32] was fundamental in developing compliant surfaces for athletics tracks that are tuned to match the “springs” in the athlete’s legs for peak performance.

There has been little work specifically related to biped robots walking on deformable surfaces, most likely because disturbance rejection for position-controlled humanoids on rigid surfaces has yet to be “solved”. There is however a significant body of work related to compliant legged locomotion, designs for adaptive deforming robots, and modeling of deformable objects for computer vision and manipulation. While generalized agile locomotion is a difficult problem, handling deformable surfaces and rough terrain are obviously a subset of that. As robots like the quadruped LittleDog and biped Atlas [33] have demonstrated, when the architecture is correct then agility is possible without prior knowledge of the terrain.

Chemori et al. used a ZMP-based Walking Pattern Generator and stabilizer, and computed torque control, to simulate the SHERPA biped walking on a compliant floor. The floor was modeled as a 3-axis spring damper system, however they don’t discuss this at length, and the legs utilize cable-driven differential-drive actuators that are lower impedance than Harmonic Drives used in most position-controlled bipeds. Also Huang et al. [34] investigated the effect of ankle compliance on a biped walking gait.

Lastly, consider the extreme example of walking on a trampoline. The reader is encouraged to try their own experiment as three modes of behavior can be observed. At a slow walking pace, there is little restitution of energy and each subsequent step is highly unstable; this is the mode of disturbance for a rigid biped robot that walks at low speed, except you can imagine a much larger destabilization because the legs are not compliant. Secondly, if the walking pace matches the natural frequency of

the trampoline, the effect is “bouncing”. Thirdly, if the walking pace is of higher frequency then the compliant legs must work very fast to maintain stability. However this thesis is concerned with a primarily rigid-body humanoid, and suddenly becoming rigid on a trampoline will result in a non-vertical reaction force which is dependent on the current state of deformation. Also the reaction force will change as the COM (Center of Mass) moves in relation to the COP (Center of Pressure). Because the foot can not be assumed to be in parallel contact with the ground plane, this violates an assumption of typical ZMP-based approaches to biped walking. This is in contrast to robots like Raibert’s hopper and Sentis’ planar biped “Hume” that have point contact feet and thus the pose of the foot does not factor.

2.4 Project Background

During 2012, the author worked at the Humanoid Robot Research Center, at KAIST (Korea Advanced Institute of Science & Technology) where they developed the KHR-1, KHR-2, KHR-3 “HUBO” and HUBO2 robot platforms. The latest iteration, the HUBO2+ is an interesting platform for research, because it is the first full-sized humanoid platform to be made available to the public. Other robots, such as Asimo and HRP, have only been conditionally leased to individual research institutions.

The HUBO2 is supplied with a Windows-based controller that enables the robot to walk by generating cyclical patterns of motion for the waist and feet based on cubic polynomials, stabilized using closed-loop feedback from FT (Force-Torque) sensors in the ankles and an IMU (Inertial Measurement Unit) in the pelvis. The current walking pattern is marginally stable so it was hypothesized that implementing a newer, model-based algorithm for generating the walking pattern, which by incorporating this knowledge of the robot dynamics, it was hoped that the stability margin could be increased such that the robot could walk around indoors without supervision.

This project is also a continuation of the author’s work in developing a real-

time Linux-based robot controller, which has previously been used to demonstrate trajectory planning on a 6 DOF manipulator [35]. This was an opportunity to test the controller's performance on a humanoid which has a much larger number of DOF and for which precise control rates are more critical than a manipulator arm. This controller was a critical component required to be able to test alternative walking algorithms on the real robot.

Experiments on the real robot were conducted at the Social Robotics Lab at A*STAR in Singapore, where they have been using a HUBO2 robot to investigate potential future applications for humanoid robots, including home security [36], in addition to promoting STEM to secondary school students. But to enable long-term, autonomous social robotics experiments in a typical home or office environment, the robot must be capable of safe and stable biped locomotion on indoor surfaces, which was the desired outcome of this project. At present, the HUBO2 must be operated with a fall-arrest harness, making such autonomous experiments impossible.

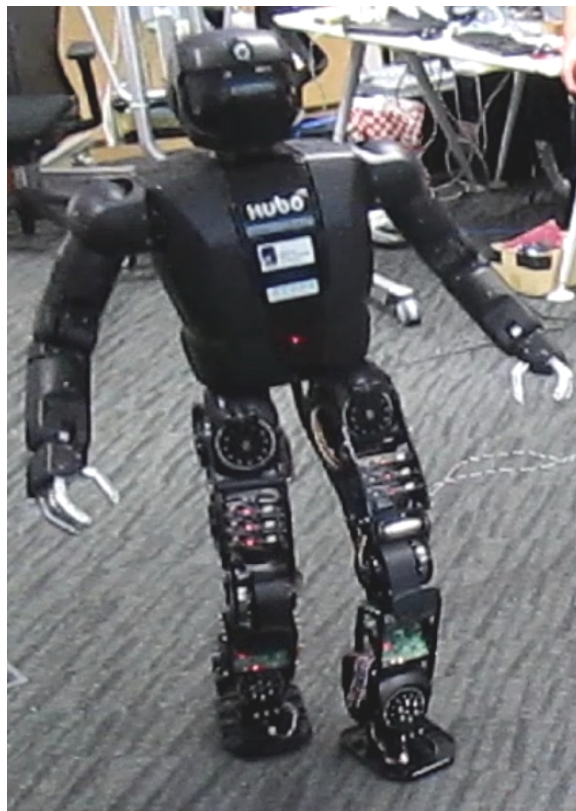


Figure 2.3: Walking test with the HUBO2 robot

Chapter 3

Methods for Robot Walking

There is a large body of research related to biped locomotion and the generation of walking patterns for humanoid robots. Specific approaches include, directly generating task space trajectories for the waist and feet using polynomials [37, 17, 38, 39], CPG (Central Pattern Generators) [40], and Fourier Series [41], or less direct approaches based on MPC (Model Predictive Control) [42, 43, 44, 45].

Walking gaits can be categorized as being; statically stable (Center of Mass inside Support Polygon), and; dynamically stable (COM outside SP, but Zero Moment Point inside SP). This may seem trivial but ZMP-based walking is predominantly statically stable. For the Parametrized Cubic Polynomial algorithm on HUBO2 the gait is approximately 80% static and 20% dynamically stable.

The most widely used criterion for ensuring the dynamic stability of a biped is the ZMP (Zero Moment Point) [8]. The ZMP is essentially the COP (Center of Pressure), and the walking pattern is designed such that the COP is maintained as close as possible to the center of a single foot, or is at least within the support polygon. These concepts are illustrated in Chap. 6.

Methods utilizing the ZMP have successfully enabled robots like ASIMO and HRP to walk, but they rely on a specific set of assumptions, being that a position-controlled humanoid has stiff rigid links, high-gain joints, and flat feet that make contact parallel to the floor. Within this class of algorithms, there are top-down

methods that calculate a stable trajectory for the COM (Center of Mass), and bottom-up methods that use the constraint of foot positions to compute a stable trajectory for the upper body. These algorithms are typically evaluated for how accurately they track the reference ZMP trajectory, which must remain strictly within the boundary of the Support Polygon.

The HUBO2 currently uses a Walking Pattern Generator that outputs a trajectory for the waist and feet in world coordinates, described by parametrized sinusoidal and polynomial functions. The walking pattern was designed offline using a simple LIPM (Linear Inverted Pendulum Model) and is stabilized online by using feedback controllers to regulate the landing of the swinging foot and to damp out unwanted oscillations. From operating the robot, it can be seen that the stability margin is low as it can easily trip and fall from the slightest disturbance, in particular while yawing the feet (turning). It was hypothesized that this was because the walking algorithm does not factor in a complete multi-body model of the robot's dynamics, nor control the ZMP at all stages of the pattern.

With the current availability of computing power, newer methods allow state of the art position-controlled humanoids to calculate a stable ZMP trajectory in real-time, which allows the HRP to perform online footstep planning [46]. These bottom-up methods are in contrast to the top-down algorithm used on HUBO, for which the foot step locations can not be directly specified because they follow the trajectory of the waist. For these reasons, this project implemented methods by Kajita [42] and Wieber [45] that use Model Predictive Control and a rigid-body model of the robot to generate a stable walking pattern to suit specific footstep positions. These methods utilizing MPC were found to be more effective than the current WPG for walking on flat surfaces, however the goal was to walk on a soft, carpet floor which was found to have sufficient deformation that it violates the "flat floor" constraint required for stable ZMP walking.

From experiments it was found that the destabilizing effect caused by walking

on a deformable surface is comparable to the robot being repeatedly pushed, so future work is to look at applying methods for “push recovery” that have been applied to solid floor surfaces. Recently, state of the art force-controlled bipeds have demonstrated stable walking under much larger perturbations using a different dynamic criteria called the “Capture Point” [28], with balance being considered as part of a whole-body motion optimization problem. Future work would be to apply these methods to a position-controlled humanoid like HUBO.

The following sections describe the existing method for generating the walking pattern, Parametrized Cubic Polynomials, along with ZMP Preview Control and Model Predictive Control that were tested on the robot. There is not much information in the literature about implementing these algorithms on a full-sized humanoid robot, so one might imagine that it is a relatively straight-forward engineering task. However, typically WPG are tested using a simple rigid-body model of the robot in simulation, walking on a solid flat floor, which does not directly scale up to a full-sized humanoid robot where unmodeled compliance can be problematic.

3.1 Parametrized Cubic Polynomials

A WPG based on cubic polynomials or sinusoids uses these functions to generate trajectories for the COM (Center of Mass) and feet of the robot. The robot is typically modeled using a LIPM (Linear Inverted Pendulum Model), with the robot’s trunk or pelvis assumed to be the position of the COM, and the trajectory parameters adjusted to create a ZMP trajectory that maintains stability. The resulting combination of the x,y trajectories for the trunk and feet of the robot creates the desired walking pattern. This method is popular because it has low computational load and so can be applied to bipeds of any capacity. A detailed explanation of applying cubic polynomials to walking patterns can be found in [47]

The HUBO2 robot currently uses a WPG that consists of linear and sinusoidal functions [37, 17], and its low complexity means it can run on a low-power Blackfin

Table 3.1: Parameters for Polynomial WPG

Parameter	Description
N_{step}	No. of steps
L_{step}	Step length
H_{step}	Step height
R_{step}	Step rotation (yaw)
D_{step}	Step direction (forward/sideways)
T_{stride}	Step period (speed)
A_{pelvis}	Hip sway amplitude
T_{delay}	Hip sway delay

Microcontroller [48]. Similarly, Xue et al. [38] developed a real-time WPG using cubic polynomials that allows the trajectory direction to be changed within a window of 1 footstep, whilst maintaining a smooth ZMP trajectory, and demonstrated it on the NAO robot. Hong et al. [39] used quartic polynomials and Least Squares method to design walking patterns that maintained smooth jerk despite a variable step length. One limitation of these algorithms is that they do not ensure the dynamic stability of the robot during walking, so feedback stabilization is required to force the robot to track the designed trajectory.

The walking pattern was designed off-line using a LIPM (Linear Inverted Pendulum Model) and then experimentally tuned and verified on the real robot. The

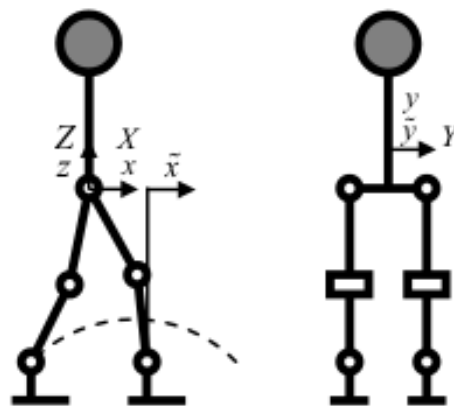


Figure 3.1: Coordinate frames for polynomial walking pattern: forward (sagittal plane) and sway (coronal plane) [17]

WPG can be described as a superposition of linear and sinusoidal functions that creates smooth, cyclic motions of the pelvis and legs. The function parameters are adjusted to create a set of walking movement primitives that allow the robot to walk forwards in increments of $0 - 20cm$, backwards $0 - 10cm$, and turn at angles of $\pm 0 - 30^\circ$.

Trajectories for the feet and pelvis are designed in body-fixed coordinates $x-y-z$ (Fig. 3.1) and then translated into world coordinates $X-Y-Z$. A FSM (Finite State Machine) is used to generate each phase of the walking pattern $\tilde{x}, \tilde{y}, \tilde{z}, y\tilde{a}w, s\tilde{w}ay$ based on the parameters shown in Table 3.1.

Using the point-mass model, a reference trajectory for the x ZMP is designed using 3rd order polynomial interpolation (3.1). The coefficients are derived from the boundary conditions, being the position and velocity at the start time $t_N = 0$ and end time $t_N = 1$ of each step [17].

$$\begin{aligned} x_{zmp} &= \sum_{i=0}^3 b_i t_N^i & (3.1) \\ &= (a_0 - 2a_2 \frac{l}{g}) + (a_1 - 6a_3 \frac{l}{g}) t_N + a_2 t_N^2 + a_3 t_N^3 \end{aligned}$$

The y ZMP trajectory is similar, but the cubic polynomial is defined piece-wise with an additional linear segment centered around $\frac{t}{2}$. This sway delay time T_{delay} holds the y ZMP position constant during the SSP (Single Support Phase), with zero velocity and acceleration.

By assuming that the location of the robot's pelvis center $x-y$ with fixed height z is the location of the COM from the LIPM, the trajectory of the pelvis will also be a 3rd order polynomial but with different coefficients. The validity of this approach and a full derivation is discussed in [17].

The x trajectory of the pelvis center is generated using the following cubic polynomial:

$$\begin{aligned}\tilde{x}_{pelvis}(t) &= \sum_{i=0}^3 a_i \left(\frac{t-t_1}{t_2-t_1} \right)^i \\ &= a_3 \left(\frac{t-t_1}{t_2-t_1} \right)^3 + a_2 \left(\frac{t-t_1}{t_2-t_1} \right)^2 + a_1 \left(\frac{t-t_1}{t_2-t_1} \right) + a_0\end{aligned}\quad (3.2)$$

where t_1 and t_2 define the time period of the swing foot between each DSP.

The y trajectory of the pelvis center is generated using 2 cubic polynomials and 1 linear segment:

$$\tilde{y}_{pelvis}(t) = \begin{cases} \sum_{i=0}^3 \bar{a}_i \left(\frac{t-t_1}{t_0-t_1} \right)^i & \text{for } t = t_1 \leq t < t_0 \\ -\beta_1 S_y & \text{for } t = t_0 \\ \sum_{i=0}^3 \bar{a}_i \left(\frac{t-t_0}{t_2-t_0} \right)^i & \text{for } t = t_0 < t \leq t_2 \end{cases}\quad (3.3)$$

noting that $t_0 = \frac{t_1+t_2}{2}$.

The x trajectory of the ankles is described by a cycloid function:

$$\begin{aligned}\tilde{x}_{ankle}(t) &= (b+f) \left(\frac{t-t_1}{t_2-t_1} - \frac{1}{2\pi} \sin \left(2\pi \frac{t-t_1}{t_2-t_1} \right) \right) - f \\ &\text{where } b = \tilde{x}_{ankle} \text{ at } t = t_1\end{aligned}\quad (3.4)$$

$$f = \tilde{x}_{ankle} \text{ at } t = t_2$$

The y trajectory of the left ankle is generated using 2 cosine segments:

$$\tilde{y}_{ankle_{left}} = \begin{cases} \frac{A}{4}(1-n) \left(1 - \cos \left(\pi \frac{t-t_1}{t_2-t_1} \right) \right) & \text{for } t = t_1 \leq t < t_0 \\ \frac{A}{4}(1-n) \left(1 + \cos \left(\pi \frac{t-t_1}{t_0-t_1} \right) \right) & \text{for } t = t_0 < t \leq t_2 \end{cases}\quad (3.5)$$

$$(3.6)$$

where n is the side-to-stride ratio and the 2nd segment is simply the first time-shifted by one half period. The right ankle is similar, but has negative A for the stride length.

3.2 ZMP Preview Control

This section will give a brief description of generating walking patterns by ZMP Preview Control [42], which uses an infinite horizon LQR (Linear Quadratic Regulator) to sample the future ZMP on a preview horizon. This method has become popular because it allows a dynamically stable trajectory to be generated online, using the desired positions of the robot's feet, which is typically the output of a planning algorithm. In contrast to the top-down approach currently used on the HUBO robot, this method is a bottom-up approach where the future footstep positions are fixed and used to compute the optimal trajectory for the robot's COM. Detailed descriptions of the algorithm can be found in [42, 43, 44, 45].

ZMP Preview has been successfully applied to full-size humanoid robots such as HRP-2 [49, 50] and Lucy [51] and toy-size humanoids including NAO and Darwin-

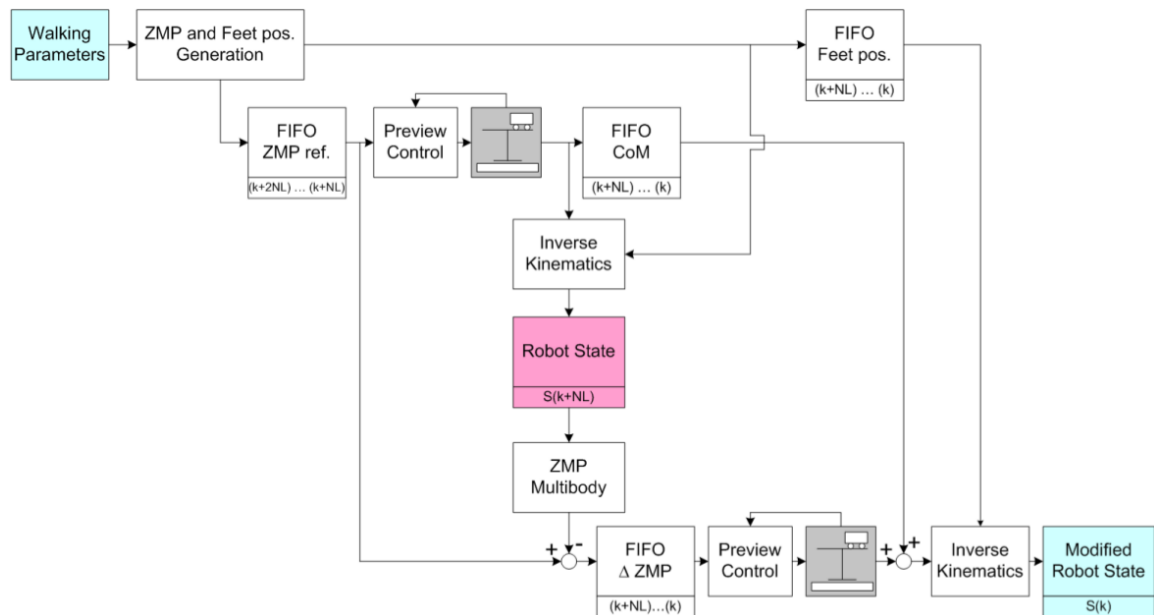


Figure 3.2: WPG using 2-stage ZMP Preview [44]

OP. Strom et al. [52] used ZMP Preview to develop an omnidirectional walking gait for the NAO and a similar WPG was developed by Aldebaran [53]. Jun et al. [54] used ZMP Preview to generate the walking pattern for a toy-sized version of HUBO called Mini-HUBO.

The original method [42] actually comprises 2-stages of ZMP Preview (Fig. 3.2), where the 2nd stage attempts to correct for the expected behavior of the full robot dynamics [55, 56]. In comparison, the toy-sized humanoids [52, 53, 54] use only the 1st stage of ZMP Preview incorporating the dynamics of the cart-table model. In one variation, [57] proposes a single-stage “General” ZMP Preview incorporating angular momentum with the cart-table dynamics.

ZMP Preview [42] has inspired an entire class of WPG that fix the footstep positions, however, these algorithms are typically tested in simulation only, where it is much easier to incorporate the current state of the robot as feedback than it is on a real robot with noisy sensor measurements. We decided to test the original ZMP Preview algorithm both because it uses a full model of the robot as a “dynamics filter”, and because of its popularity, to determine how effective the method is on a full-sized robot. A quick overview of the algorithm is provided here.

Using the 3D-LIPM to model the robot dynamics, the COP (Center of Pressure) in the forward direction is:

$$p_x = x - \frac{z_c}{g} \ddot{x} \quad (3.7)$$

for which the inputs are the forward position of the COM x , acceleration of the COM \ddot{x} , constant height of the COM z_c , and constant gravity g . However ZMP Preview solves the inverse problem for which the COP is an input. Note the COP equations are decoupled and so the equation for the lateral direction p_y is similar [42].

As with the Polynomial WPG, the trajectories for the COP and COM are described by 3rd order polynomials.

A discretized system with constant sampling period T is developed [42] such that:

$$\hat{x}(k+1) = \begin{bmatrix} 1 & T & \frac{T^2}{2} \\ 0 & 1 & T \\ 0 & 0 & 1 \end{bmatrix} \hat{x}(k) + \begin{bmatrix} \frac{T^3}{6} \\ \frac{T^2}{2} \\ T \end{bmatrix} \ddot{x}(k) \quad (3.8)$$

where the state of the system is:

$$\hat{x}(k) = \begin{bmatrix} x(kT) \\ \dot{x}(kT) \\ \ddot{x}(kT) \end{bmatrix} \text{ for } k = 1, 2, \dots \quad (3.9)$$

and the system input is the time-derivative of the acceleration of the COM (the jerk):

$$\ddot{\ddot{x}} = \frac{d}{dt} \ddot{x} \quad (3.10)$$

The goal is that each footstep is constrained to a certain position on the ground and ideally the COP is located at the center of the foot. ZMP Preview attempts to track this desired COP by minimizing the jerk, which can be solved using a QP (Quadratic Program) [45]:

$$\min_{\ddot{x}(k), \ddot{x}(k+1), \dots} \sum_{i=k}^{\infty} \frac{1}{2} Q (p_x(i+1) - p_x^{ref}(i+1))^2 + \frac{1}{2} R \ddot{\ddot{x}}^2(i) \quad (3.11)$$

with constant weights Q and R .

At each step, the resultant COM position is used as the position of the pelvis center. Using IK (Inverse Kinematics) the current state and ZMP of a full dynamic model of the robot is computed. This expected ZMP is then fed into a 2nd Preview stage to calculate a refined trajectory for the COM and the updated state commands are sent to the robot.

The original ZMP Preview method requires much more computing power than

the Polynomial WPG, hence why a simplified version is used for robots with small on-board processing capabilities like NAO. Similarly for full-size humanoids like HUBO2, experience has shown that it is best to design with minimum 2 CPU cores for generating the critical real-time robot motions.

There is some time delay required to compute the gains for the Preview Controller and the length of the initial Preview Horizon. This means that in its current form it is not feasible to change the desired footstep locations inside the preview window period. This problem has been examined in [50, 58].

3.3 Model Predictive Control

ZMP Preview [42] has inspired various improved methods for generating walking patterns, including optimization for speed [59] and fast online change of footstep positions [60, 58]. This section will briefly describe Wieber's method [45] that effectively extends ZMP Preview to have explicit bounds on the trajectory of the ZMP, making it robust against external disturbances.

Wieber [45] proposed solving the Quadratic Program for ZMP Preview (3.11) on a finite time horizon using Model Predictive Control:

$$\min_{\ddot{x}(k), \dots, \ddot{x}(k+N)} \sum_{i=k}^{k+N-1} \frac{1}{2} Q (p_x(i+1) - p_x^{ref}(i+1))^2 + \frac{1}{2} R \ddot{x}^2(i) \quad (3.12)$$

and also proposed a reformulation of this QP (3.12) with constraints on the ZMP:

$$\min_{\ddot{x}(k), \dots, \ddot{x}(k+N)} \frac{1}{2} \ddot{x}^2(k) \quad (3.13)$$

$$z_{k(min)} \leq z_k \leq z_{k(max)}$$

which ensures that the controller will keep the COP within a small, safe region of the support polygon, even when the walking pattern is disturbed by an unexpected

external force.

This QP is solved analytically using an off-the-shelf solver. Given that a solution to the QP (3.13) must be computed at each time step, a WPG using this Model Predictive method will need sufficient computing power to solve the QP (3.13) at each time step, however [60] demonstrated a specialized solver with significantly faster speed.

Chapter 4

Simulation Environment

4.1 Physics Simulators

A dynamic simulation of the HUBO2 robot was created, both to verify the new walking algorithms and because the actual robot was only available for 4 weeks of testing.

There are numerous software packages for simulating dynamic behaviour of multi-body objects, but currently the differentiating features that are required to model a humanoid robot but are not broadly available, are:

- Accurate computation of force and contact constraints - important for simulating a biped robot
- Ability to apply a force to the robot - a “push”
- 6-axis Force-Torque sensor - used on the ankles of biped robot
- A ball joint with spring-damper - to model compliant ankle joint
- Ability to record absolute position of robot’s links
- Import STL mesh for visuals (optional)
- Slider joint, for humanoid head (optional)

- Kinect sensor with ROS PointCloud output, for perception (optional)
- Ability to model articulated fingers of a hand (optional)

The most popular physics engines for simulating robots are:

Table 4.1: Physics Engines

Physics Engine	Solver	Speed	Accuracy	Ease of Use	Cost
ODE [61]	Iterative	6/10	6/10	7/10	Free
Bullet [62]	Iterative	8/10	7/10	7/10	Free
Vortex [63]	unknown	unknown	9/10	unknown	Expensive

The ratings in Table 4.1 are somewhat subjective, but it highlights that Bullet is known to have faster computation speed than ODE (Open Dynamics Engine), due to numerous code optimizations, and the accuracy of simulations are typically slightly more accurate than ODE, with less “parameter tweaking” required. Vortex provides even more accurate results and advanced capabilities, but was too expensive for this project.

While it is possible to directly use one of these Physics Engine to develop a dynamic simulation from scratch, it is best to leverage a complete software simulation program, such as:

Table 4.2: Robot Simulation Software

Software Package	Physics Engine(s)	Accuracy	Ease of Use
Gazebo [64]	ODE, Bullet (limited)	6/10	5/10
OpenRAVE [65]	ODE, Bullet	6/10	4/10
V-REP [66]	ODE, Bullet, Vortex (non-free)	7/10	6/10
<i>Webots</i> [67]	<i>ODE</i>	<i>6/10</i>	<i>7/10</i>
Morse [68]	Bullet	unknown	4/10
OpenHRP [69]	Custom (Featherstone)	8/10	4/10

It would be interesting to analyse the computational complexity (Big-O) of the algorithms used in each software package, however a simulation environment will use multiple systems for constraint solving and collision checking, and so typically some

metric is established (i.e. compute time for 5000 falling boxes) and comparisons made in that fashion. However, for biped walking, simulation accuracy is more important than speed.

Webots was used to develop the simulation, as it includes all of the required features in the above list, the author had previous experience using Webots, and there was limited time available to learn a new tool. Some testing was performed in OpenHRP, which has been used to create accurate simulations for the HRP and DLR bipeds, however the documentation is poor and the user base is small, which made troubleshooting time consuming. Future work will look at using V-REP, which has more features and the recently added Vortex physics engine and the soon to be released Bullet 3.x look promising.

4.2 Robot Model

The simulation model was created using inertial properties of the robot obtained from CAD data. The HUBO2+ robot has 38 DOF and weighs 45kg in total. Critical dimensions for the lower-body are shown in Fig. 4.1, with the size of the feet being $0.22 \times 0.15m$.

In an upright straight-legged pose the height of the COM is $COM_z = 0.645m$. When the robot moves to a stable bent-knee pose the $COM_z = 0.6146m$, for joint angles:

$$\theta_{hip\ pitch} = -21.8^\circ$$

$$\theta_{knee} = 43.6^\circ$$

$$\theta_{ankle\ pitch} = -21.8^\circ$$

The real robot uses high-gain PID joint controllers, so these are modeled in the simulation as position-controlled revolute joints with essentially infinite gain. The robot's body is modeled using simplified geometric shapes (squares and cylinders)

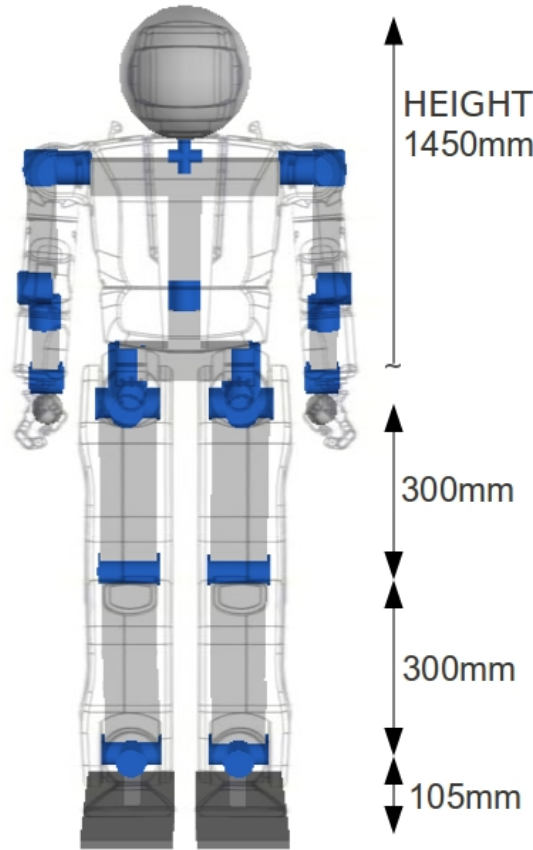


Figure 4.1: Simulation model of the HUBO2 robot

for the visual appearance, which speeds-up computation. The same geometry is used for collision detection, which is not performed between adjacent links so that complex geometry is not required in the area of the joint. The robot has a compliant, urethane bushing in the ankle for vibration damping, which is modeled by a spherical (ball) joint with variable spring parameter k .

On the simulated robot, single-axis force sensors are positioned on the corners of the feet, which allows computation of the COP (Center of Pressure):

$$x_{cop} = \frac{\sum_{i=1}^8 (F_{zi} p_{xi})}{\sum_{i=1}^8 F_{zi}} \quad (4.1)$$

$$y_{cop} = \frac{\sum_{i=1}^8 (F_{zi} p_{yi})}{\sum_{i=1}^8 F_{zi}} \quad (4.2)$$

where p_{xi} and p_{yi} are the distance of the i^{th} force sensor from the respective ankle.

The real robot has a Force-Torque in each ankle, between the urethane bushing

and the foot, which measures the downward force F_z and moments M_x and M_y which are used to compute the ZMP (Zero Moment Point). Webots does not have a specific sensor for measuring torque, so a dummy joint was added to the simulation model and an ODE physics plugin is used to extract the forces and torques that satisfy the joint constraint during each iteration of the simulation.

Using the force-torque data and assuming a simple Cart-Table model [42] for the robot, the ZMP in the x and y direction is:

$$p_x = \frac{-\mathcal{T}_y}{F_z} \quad (4.3)$$

$$p_y = \frac{\mathcal{T}_x}{F_z} \quad (4.4)$$

where \mathcal{T}_x and \mathcal{T}_y are the ankle torques, and F_z is the force acting in the vertical direction.

From ODE we can also extract the current COM (Center of Mass) for each link, at each time step, and calculate the robot's overall COM:

$$r_G = \frac{\sum_{i=1}^{40} r_i m_i}{\sum_i^{40} m_i} \quad (4.5)$$

where r_i is the position and m_i is the mass of the i^{th} link.

The location of contact points between the feet and the floor are extracted, and the convex hull calculated using the Graham Scan algorithm. OpenGL is used to visually display the location of the COP, ZMP, COM and Support Polygon.

4.3 World Model

Various simulated worlds were modeled to suit specific experiments.

Fig. 4.2 shows a typical indoor environment where the robot encounters an obstacle on the ground and must walk around it, whilst maintaining stability. This was used as a benchmark because the sharp turns can easily destabilize the current

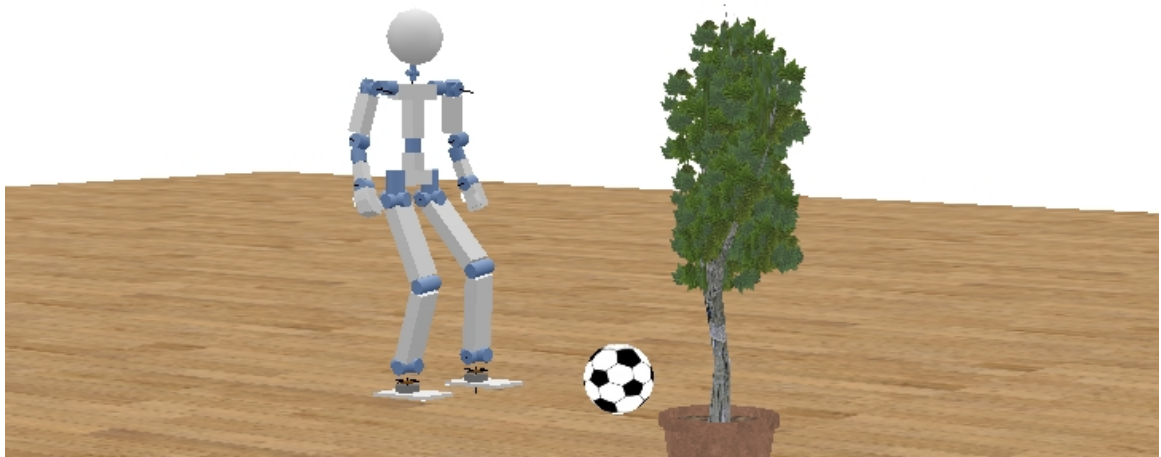


Figure 4.2: Simulated HUBO2 robot walking around obstacles

Walking Pattern Generator.

Other experiments compared walking on a solid rigid floor to a deformable floor. Fig. 7.1 in Chap. 7 shows a floor that was modeled with special interchangeable segments, with one segment having a comparatively larger CFM (Constraint Force Mixing) parameter. Normally collisions between solid bodies are modeled as rigid contacts, but varying the CFM has the effect that when the robot walks on this segment of floor its foot will be absorbed into the floor by a variable amount.

4.4 Model Validation

If the simulation model does not produce comparable behaviour to the real robot then it is no better than a computer game. Previous work has validated the behaviour of the HRP-1 robot taking a step in the real world compared to the OpenHRP simulator [70], and a real HOAP-2 humanoid compared to simulation in Webots [71].

The downward force acting on the Force-Torque sensors in the ankles of the real HUBO2 robot is comparable to the simulation model:

Unfortunately there was insufficient time to record a detailed log of force-torque data while the real robot was walking, however the dynamic behaviour was quali-

Table 4.3: Comparison of downward force acting on each ankle in static position

	Force F_z
Real Robot	200-200 N
Simulation	180 N

tatively compared. Fig. 4.3 is a screen capture from a video clip included on the accompanying CD. When the robot is modeled as a perfectly rigid system, neglecting the compliance in the ankle and foot, the robot can walk perfectly in simulation without feedback control, which is unrealistic. When the ankle is modeled with a spherical joint with spring constant $k = 500$ the simulated behaviour is more realistic.

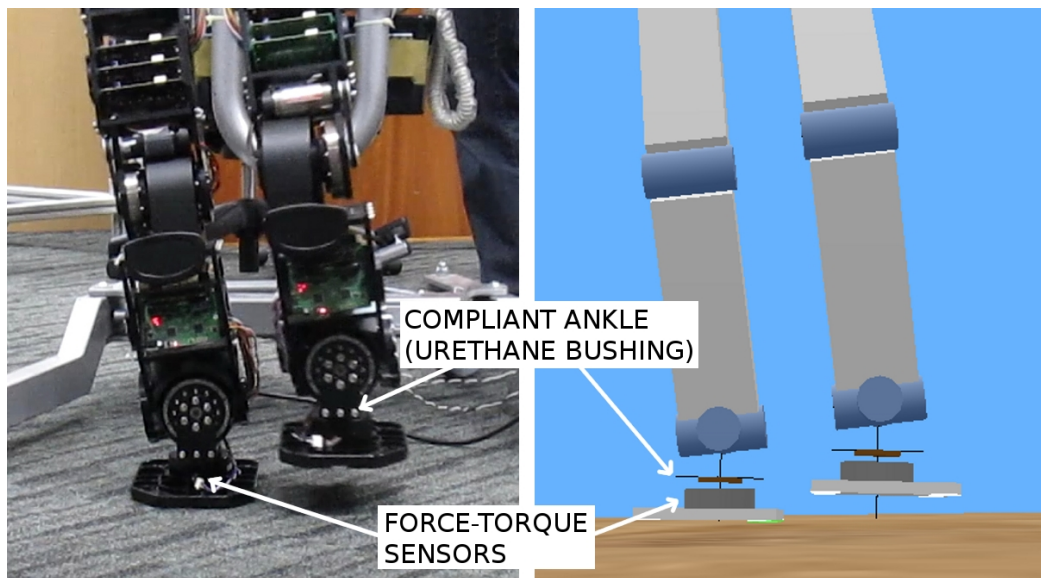


Figure 4.3: The compliant joint in the ankle of the real robot is modeled with a sprung ball joint

Chapter 5

Robot Controller

The real robot uses a software control system written in C++ and running on Ubuntu Linux, combined with the Xenomai framework for hard real-time performance. Various software libraries are used, including JRL-Dynamics to create the representation of the robot. The computer supplied with the robot is an Advantech PCM-3362 Embedded PC with single-core Atom N450 CPU.

The walking algorithms were initially tested with the Webots simulation, then tested on a separate control PC which had been removed from the robot. The controller is linked to ROS (Robot Operating System) for higher-level functionality, which is also used to verify the walking algorithm is working correctly before testing



Figure 5.1: Embedded PC removed from robot, for testing the control software

on the real robot. The control loop runs in real time and a kinematic visualization of the robot is displayed in ROS Rviz, which can reveal software bugs like math errors that produce kinematic singularities.

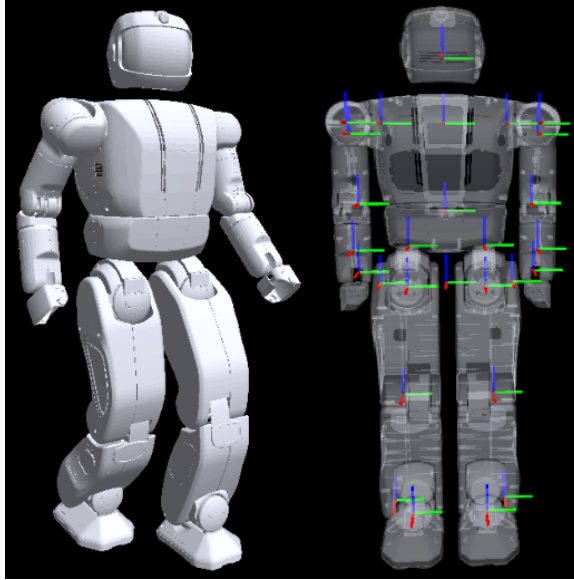


Figure 5.2: HUBO2 visualization in ROS receives joint commands from Control PC

Chapter 6

Walking Stability

During simulation, the position of the COM (Center of Mass), GCOM (Ground Projection of the Center of Mass), ZMP (Zero Moment Point), COP (Center of Pressure) and SP (Support Polygon) are recorded, as shown in Fig. 6.1.

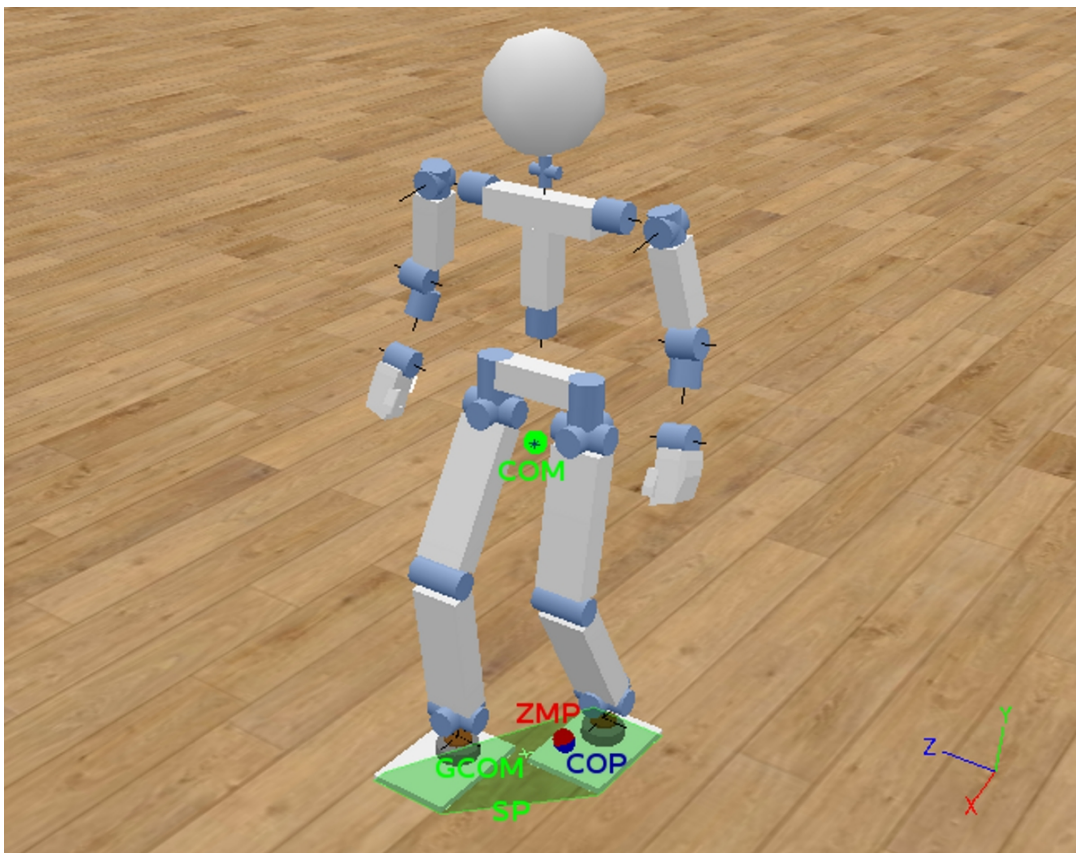


Figure 6.1: Stability metrics for a humanoid robot

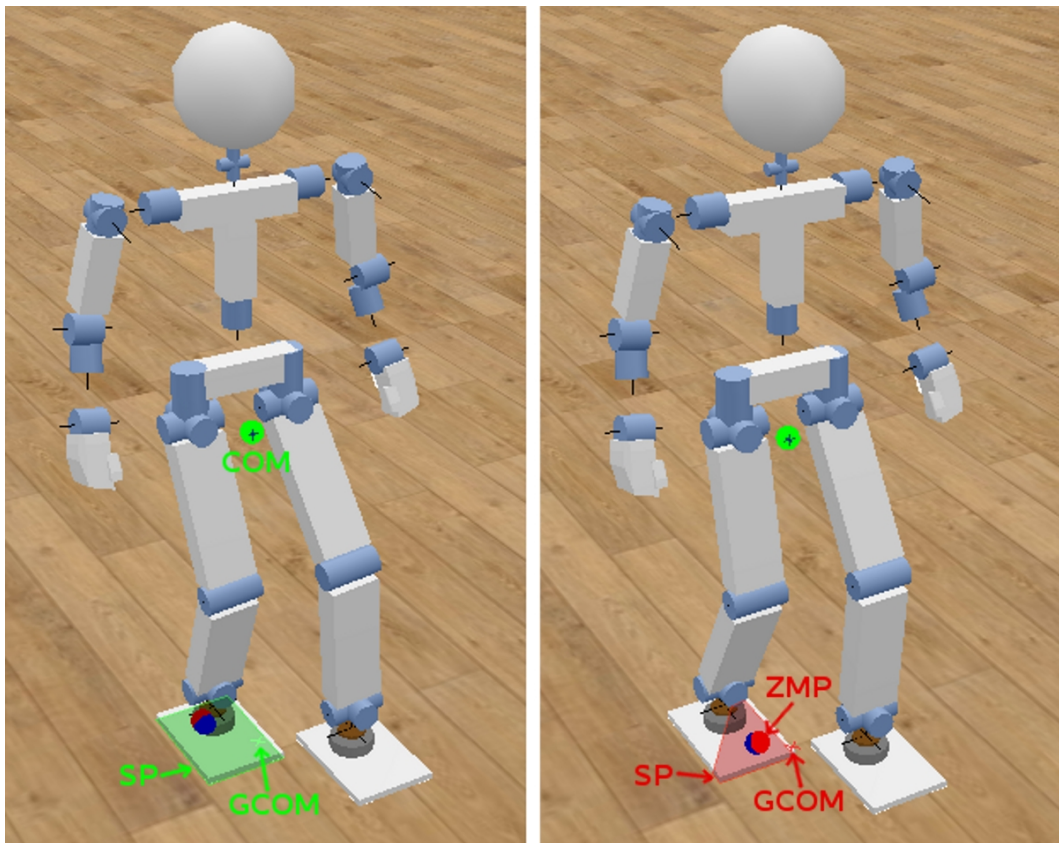
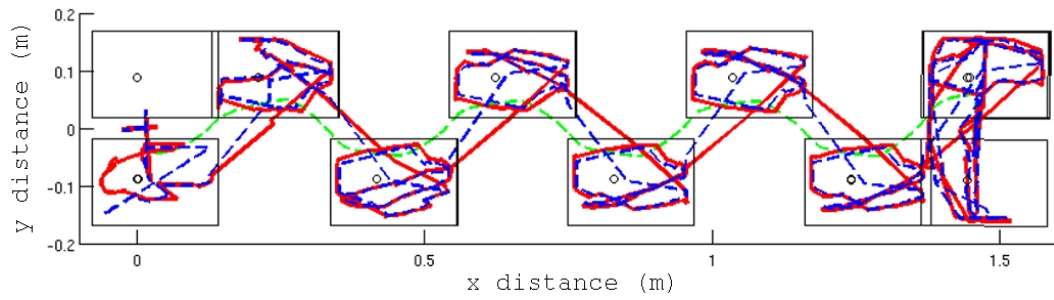
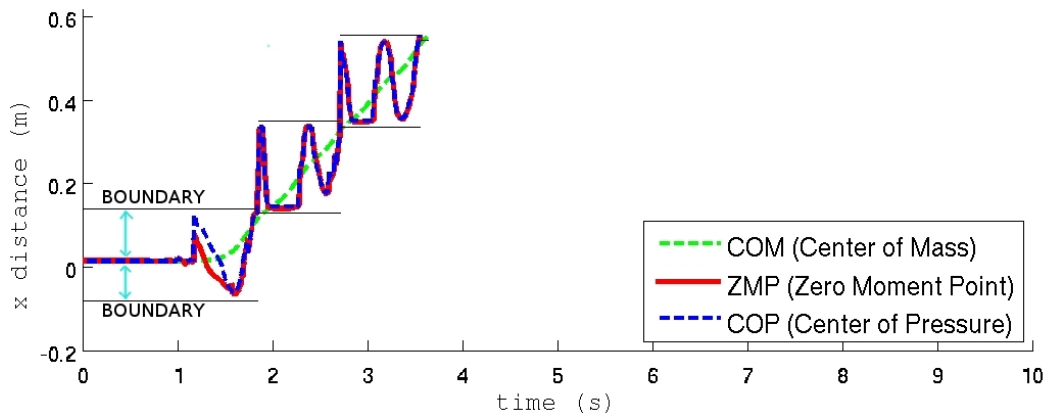
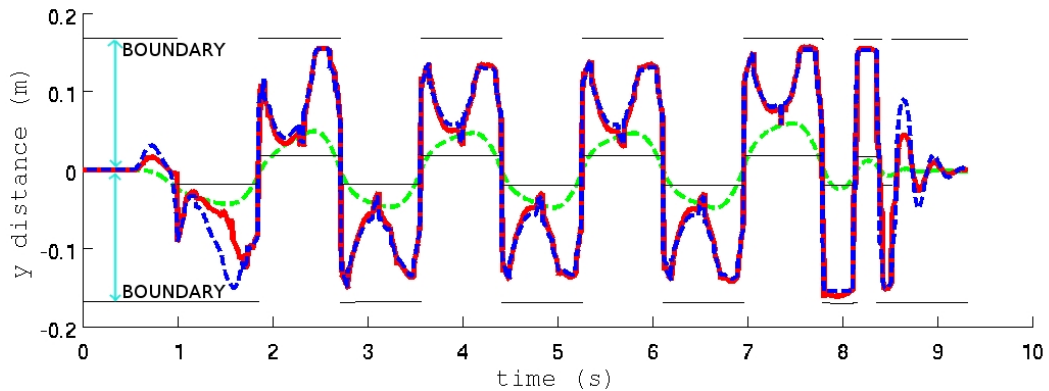


Figure 6.2: Left: Statically stable, GCOM is inside the SP.
 Right: Dynamically stable, the GCOM is outside the SP,
 but the ZMP is inside the SP.

As mentioned in Chap. 3, if the GCOM is inside the SP, then the robot is statically stable (left of Fig. 6.2). If the GCOM is outside the SP then the robot is not statically stable (right of Fig. 6.2). However, the robot can be considered dynamically stable if the ZMP is within the SP, which is called the ZMP Stability Criterion.

For this project, the stability of the robot is specifically the minimum absolute distance between the ZMP and the edge of the SP. Fig. 6.3 shows the evolution of data collected through time, for a typical experiment where the robot walks in a straight line. Initially the robot is in DSP (Double Support Phase) with the feet together, then SSP (Single Support Phase) with a left step, then a right step, and so on. For maximum stability, the ZMP should be in the center of the foot during SSP, however from the graph it can be seen that the robot has marginal stability in

Figure 6.3: Evolution through time of COM, ZMP COP in the $x - y$ planeFigure 6.4: Fore-aft stability margin, x distance between ZMP and SPFigure 6.5: Lateral stability margin, y distance between ZMP and SP

places where the ZMP is close to the edge of the foot outline.

Fig. 6.4 highlights the fore-aft stability in the x direction, where the stability margin (blue arrows) is the distance between the ZMP and the front/rear of the support polygon. Similarly, Fig. 6.5 highlights the lateral stability in the y direction, where the stability margin is the distance between the ZMP and the left/right of the support polygon.

Chapter 7

Experiments

7.1 Testing the new WPG

The three Walking Pattern Generators were used to make the simulated robot walk 6 steps in a straight line, and to follow a more difficult trajectory where the robot must turn to avoid an obstacle (Fig. 4.2). The WPG were also used to test a short 4 step footstep pattern on the real robot.

7.2 A Compliant Floor

The simulated robot was made to walk on a rigid floor, but where the floor at the location of the 3rd foot step is compliant and deforms downwards when the robot steps on it (Fig. 7.1).

7.3 Impulse Disturbance

Again, the simulated robot was made to walk on a rigid floor, but on the 3rd foot step the robot receives an impulsive force on the chest link (Fig. 7.1), as if someone pushed it.

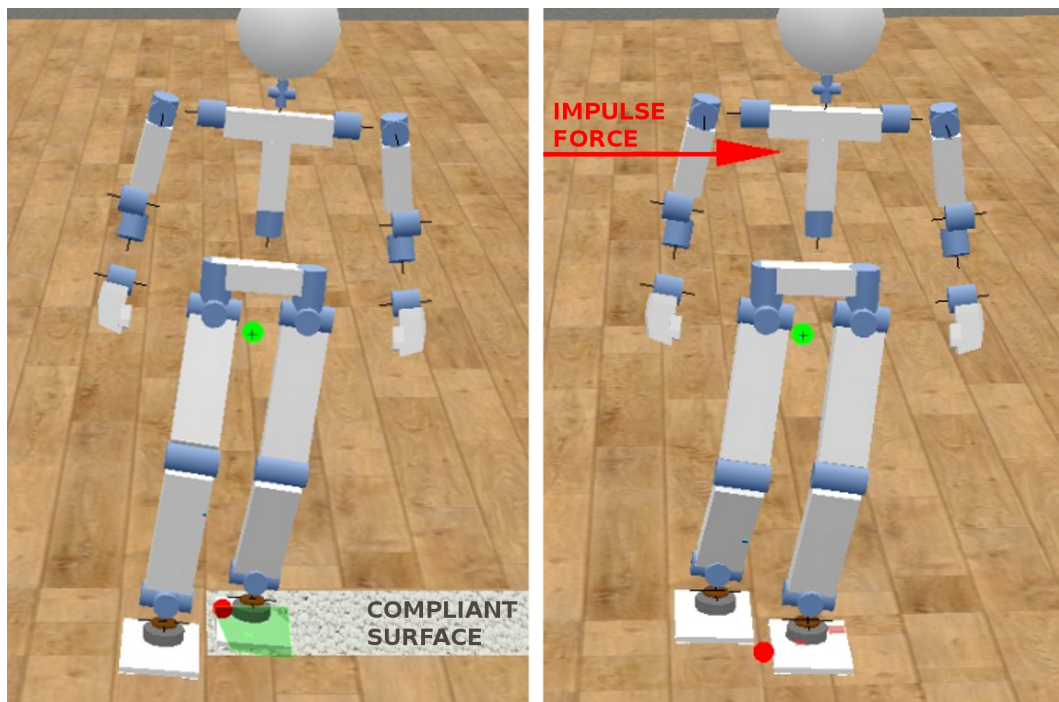


Figure 7.1: Left: Robot makes one step on compliant surface.
Right: Robot is pushed while mid-step.

Chapter 8

Results and Discussion

8.1 New Walking Pattern Generator

The walking patterns generated by the simulated robot whilst avoiding an obstacle are shown in Fig. 8.1 – 8.3, using the Cubic Polynomial, ZMP Preview and MPC-based algorithms. The actual COP (Center Of Pressure) and COM (Center of Mass) of the simulated robot are overlaid on the footstep pattern. For clarity, only the COP is shown in this chapter because it is conceptually easier to understand and is equivalent to the ZMP when the robot is dynamically stable.

The walking pattern generated using Cubic Polynomials is stable in simulation, but the stability margin is lower than the other methods, particularly while executing a turn. The ZMP Preview and MPC methods have a higher stability margin which results in a more stable walking pattern in simulation. This is due to the incorporation of the robot's dynamic model, and the MPC method is slightly better because the algorithm actually imposes constraints on the ZMP margin. In both cases there is some lateral and forward pitching of the COP which is due to inaccuracies in how Webots/ODE models the solid contact between the feet and floor.

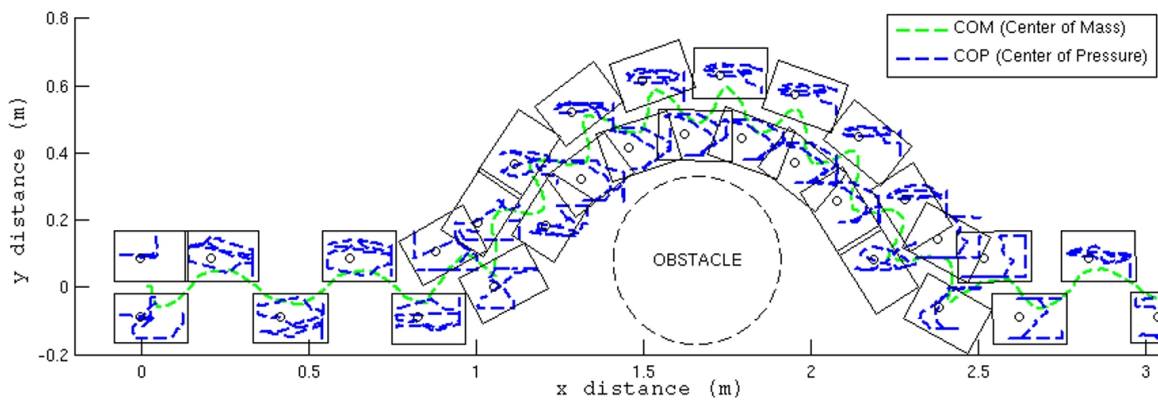


Figure 8.1: Footstep path & evolution of COP whilst walking around obstacle, using Polynomial WPG in simulation

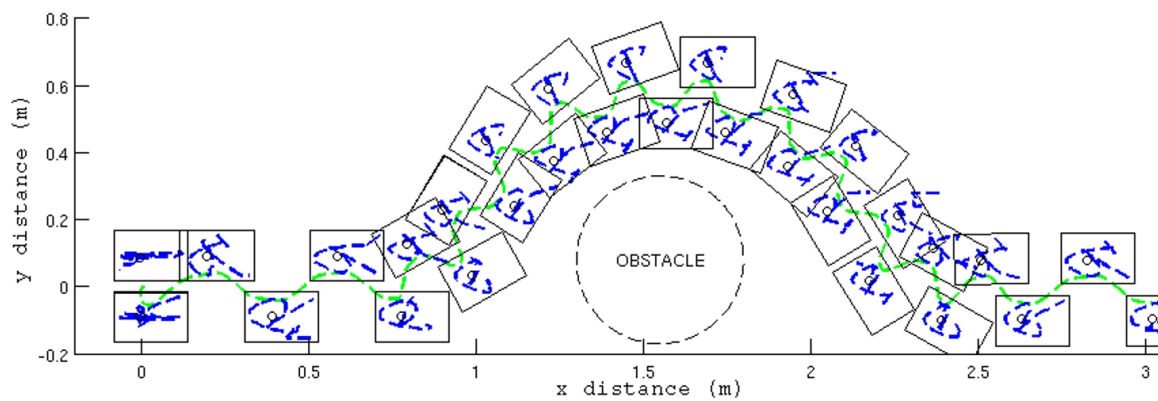


Figure 8.2: Footstep path & evolution of COP whilst walking around obstacle, using ZMP Preview WPG in simulation

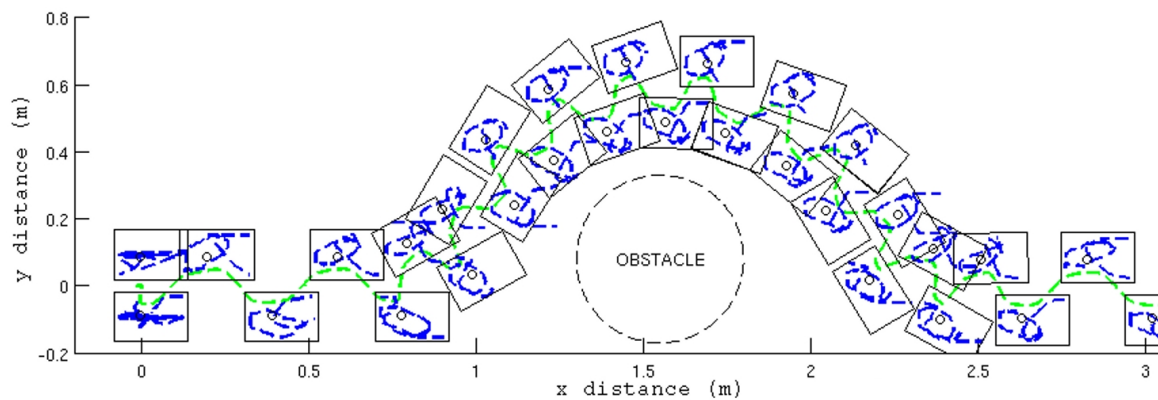


Figure 8.3: Footstep path & evolution of COP whilst walking around obstacle, using MPC WPG in simulation

8.2 Testing on the Real Robot

The WPG (Walking Pattern Generators) were tested on the real robot with a short 4 step pattern. The robot exhibited similar behavior to the simulation, although unfortunately raw data could not be collected. The shock loads induced on the stiff joints from contact with the floor can damage the Harmonic Drive units and causes the encoders to slip a few ticks, requiring regular re-alignment of the joints.

The ZMP Preview method assumes that the robot's feet always make contact parallel to the floor, and there are no strict boundaries on the ZMP, so this method is not applicable to a deformable surface. The MPC method applies a strict constraint to the ZMP and has previously showed the ability to compensate for a push disturbance, in simulation. Unfortunately there was insufficient time to implement the required closed-loop feedback from the robot, but if successful this would confirm that this method for push recovery is applicable to walking on a deformable surface.

8.3 Deformable Floor and a Push

Fig. 8.4 and 8.5 compare the effect on the COP after the simulated robot steps onto a deformable surface, and subjected to an impulse force. Both show a decrease in lateral stability because the rigid-body robot effectively becomes like a pendulum rocking back and forth. The deformable surface induces a rocking motion and lower stability in the fore-aft direction, and a slight twisting motion, due to the varying angle of contact on the foot surface.

Fig. 8.6 – 8.8 compare the lateral (y axis) stability margin while walking on a rigid floor, stepping onto a deformable surface, and subjected to an impulse force.

Fig. 8.9 compares the effect on the lateral stability for stepping onto the deformable surface in relation to the amount of compliance, which is specified by the contact parameter *SoftCFM*. The circle highlights the divergence for increasing

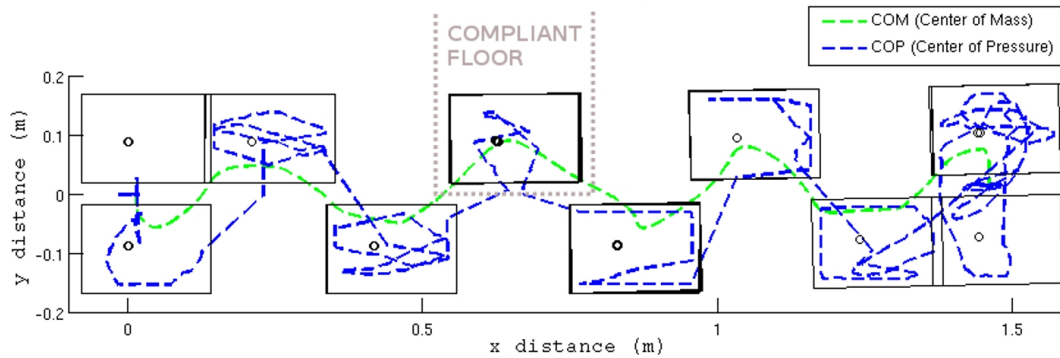


Figure 8.4: Robot makes one step on compliant surface, footstep path & evolution of COP in simulation

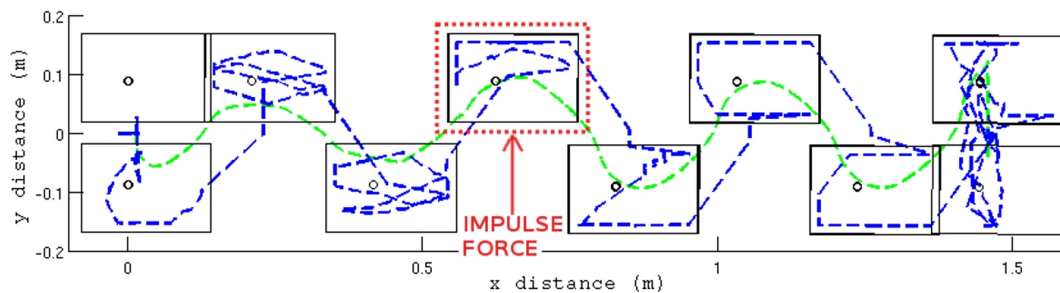


Figure 8.5: Robot is pushed while mid-step, footstep path & evolution of COP in simulation

amount of deformation in the floor, with $SoftCFM = 0.019$ causing the underactuated robot to topple over. This is the threshold push disturbance, for which below the robot could be stabilized by controlling the ankle such that parallel foot-to-floor contact is returned, and for which above the robot would require a whole-body stabilizer that would control the upper body to create a counter moment.

Fig. 8.10 illustrates the effect of a push compared to a deformable floor.

In summary, a push will cause a tipping moment about the edge of the foot which makes the robot underactuated, and on a deformable surface when the COM moves over the COP the robot is similarly underactuated as the flat foot rolls on the changing contour of the surface. For floors with a small amount of compliance, the rolling effect is negligible and some damping could be useful if the robot did not

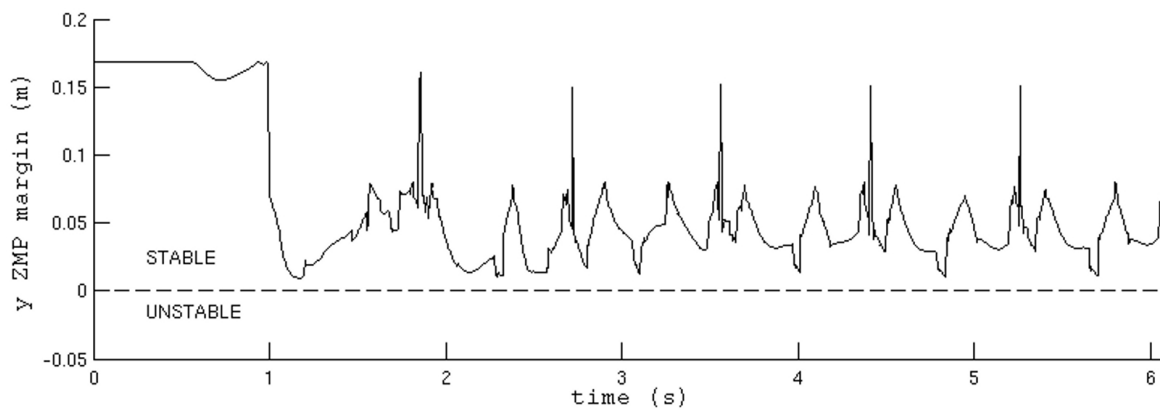


Figure 8.6: Lateral stability margin (y ZMP) while walking on rigid floor

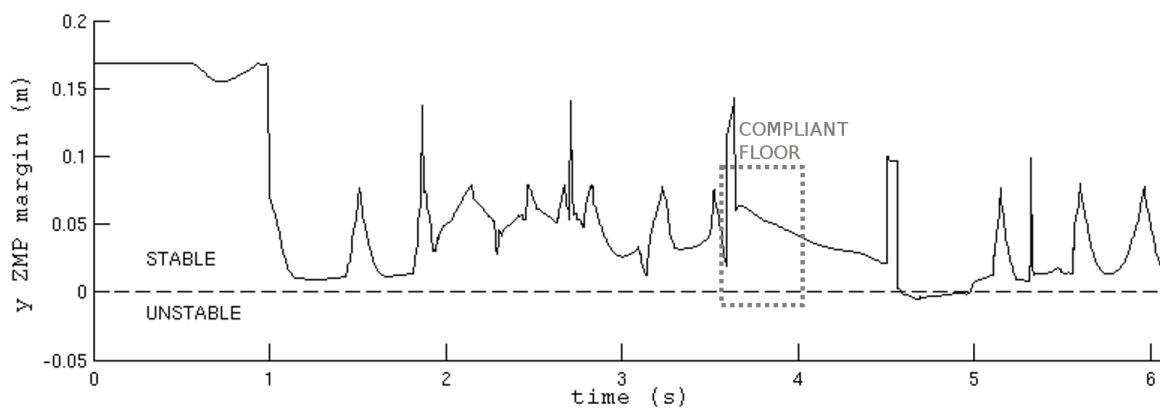


Figure 8.7: Lateral stability margin (y ZMP) with deformable floor segment

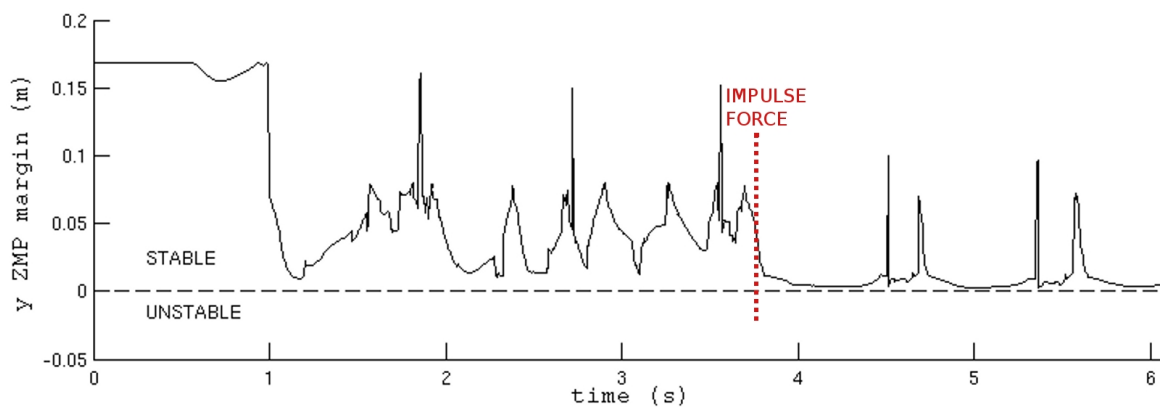


Figure 8.8: Lateral stability margin (y ZMP) with a push

already have compliance built into the foot and ankle. For surfaces with significant deformation, which is the focus of this study, the rolling effect induces greater lateral and fore-aft instability.

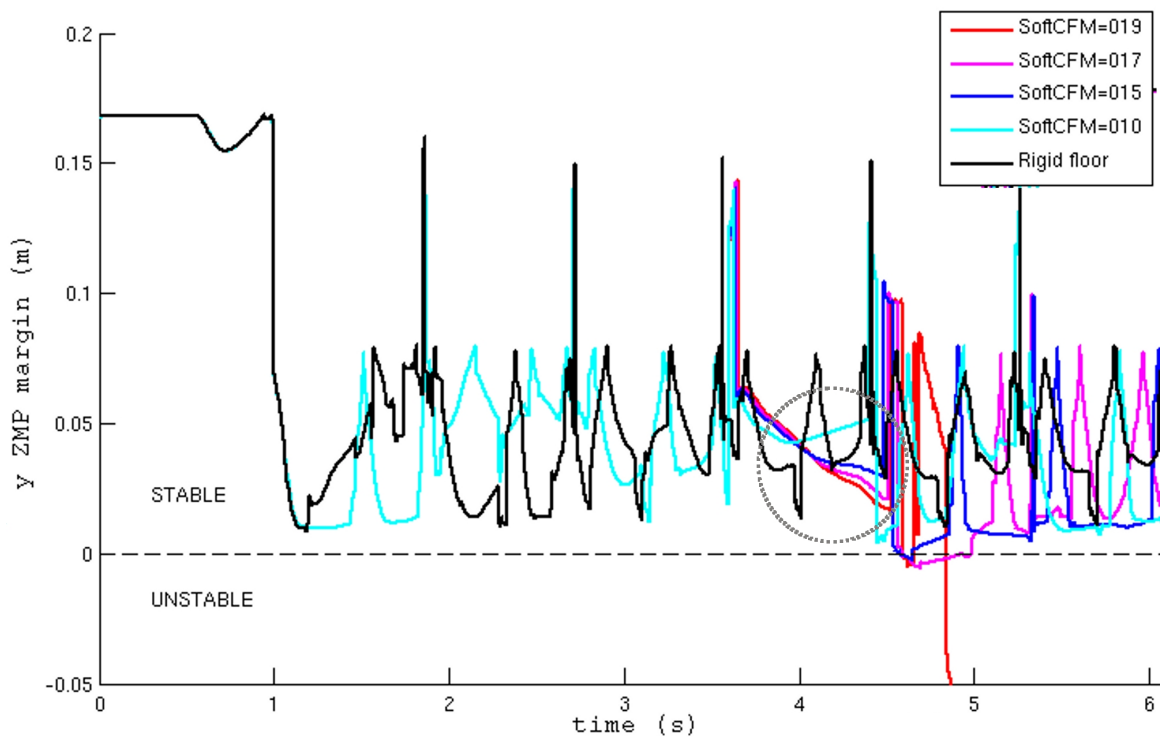


Figure 8.9: Lateral stability (y axis) for floor segment with increasing deformation (SoftCFM) in simulation

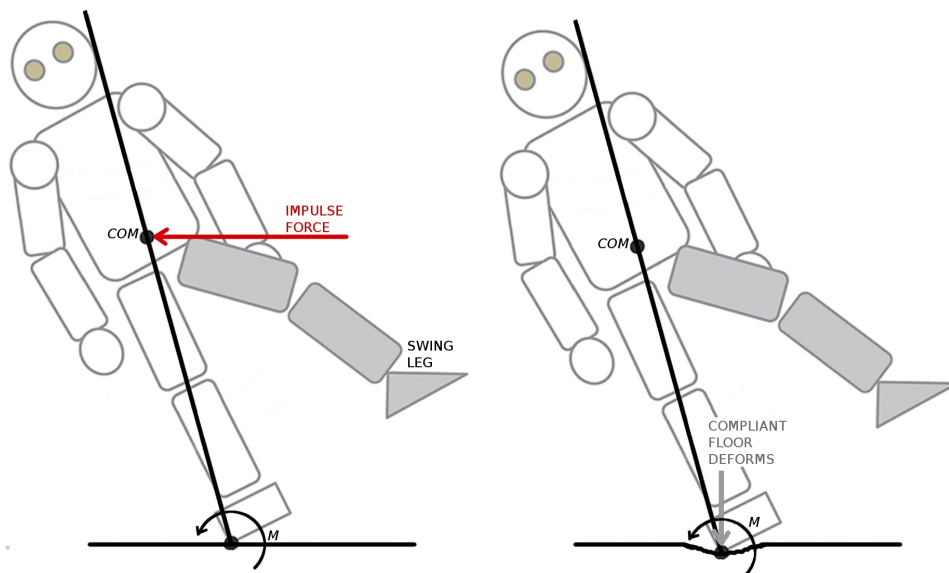


Figure 8.10: When the rigid biped is pushed, a tipping moment acts on the edge of the foot making the robot underactuated (left). A highly deformable floor will also destabilize the robot and induce a similar tipping moment.

8.4 Conclusions

For a stiff position-controlled biped, the resultant destabilizing effect of walking on a deformable surface is comparable to the effect of the robot being pushed, which is a tipping moment about the edge of the foot that makes the robot underactuated. Two potential approaches for balance control on a deformable surface are suggested; Firstly, to develop a much more complex system that incorporates a non-rigid robot model and a detailed model of the floor surface. It is easy to imagine that such methods would become inordinately complex as the robot is used in increasingly complex environments. Secondly, to use a Walking Pattern Generator based on a simple LIPM (Linear Inverted Pendulum Model) but incorporating the linear and angular momentum, combined with a whole-body controller that can manipulate the upper body to maintain stability.

Bibliography

- [1] P. Oh. (2010) Lecture by paul oh: Robotics, pathways to transformative research. [Online]. Available: www.youtube.com/watch?v=QSR30-IMaZM
- [2] Ekso bionics. California, United States. [Online]. Available: <http://www.eksobionics.com/eksohope>
- [3] Rex bionics ltd. Auckland, New Zealand. [Online]. Available: www.rexbionics.com/aboutrex.php
- [4] Vanderbilt university bionic leg. [Online]. Available: www.gizmag.com/vanderbilt-bionic-leg/20264/
- [5] I. S. A. Blog. (2012, November) Where are the elder care robots? [Online]. Available: <http://spectrum.ieee.org/automaton/robotics/home-robots/where-are-the-eldercare-robots>
- [6] ——. (2013, July) Honda developing disaster response robot based on ASIMO. [Online]. Available: <http://spectrum.ieee.org/automaton/robotics/humanoids/honda-new-disaster-humanoid-robot>
- [7] T. D. A. R. P. A. DARPA. (2012, April) DARPA robotics challenge (DRC). [Online]. Available: http://www.darpa.mil/Our_Work/TTO/Programs/DARPA_Robotics_Challenge.aspx

- [8] M. Vukobratović and B. Borovac, “Zero-moment point - thirty five years of its life,” *International Journal of Humanoid Robotics*, vol. 1, no. 1, pp. 157–173, 2005. [Online]. Available: <http://www.cs.cmu.edu/~cga/legs/vukobratovic.pdf>
- [9] Y. Sakagami, R. Watanabe, C. Aoyama, S. Matsunaga, N. Higaki, and K. Fujimura, “The intelligent asimo: system overview and integration,” in *Intelligent Robots and Systems, 2002. IEEE/RSJ International Conference on*, vol. 3, 2002, pp. 2478–2483 vol.3.
- [10] Y. Ogura, H. Aikawa, K. Shimomura, A. Morishima, H. ok Lim, and A. Takanishi, “Development of a new humanoid robot wabian-2,” in *Robotics and Automation, 2006. ICRA 2006. Proceedings 2006 IEEE International Conference on*, 2006, pp. 76–81.
- [11] K. Nishiwaki, T. Sugihara, S. Kagami, F. Kanehiro, M. Inaba, and H. Inoue, “Design and development of research platform for perception-action integration in humanoid robot: H6,” in *Intelligent Robots and Systems, 2000. (IROS 2000). Proceedings. 2000 IEEE/RSJ International Conference on*, vol. 3, 2000, pp. 1559–1564 vol.3.
- [12] S. Kagami, K. Nishiwaki, J. Kuffner, J.J., Y. Kuniyoshi, M. Inaba, and H. Inoue, “Online 3d vision, motion planning and bipedal locomotion control coupling system of humanoid robot: H7,” in *Intelligent Robots and Systems, 2002. IEEE/RSJ International Conference on*, vol. 3, 2002, pp. 2557–2562 vol.3.
- [13] K. Kaneko, F. Kanehiro, S. Kajita, H. Hirukawa, T. Kawasaki, M. Hirata, K. Akachi, and T. Isozumi, “Humanoid robot hrp-2,” in *Robotics and Automation, 2004. Proceedings. ICRA '04. 2004 IEEE International Conference on*, vol. 2, 2004, pp. 1083–1090 Vol.2.

- [14] F. Pfeiffer, K. Löffler, and M. Gienger, “The concept of jogging johnnie,” in *Robotics and Automation, 2002. Proceedings. ICRA '02. IEEE International Conference on*, vol. 3, 2002, pp. 3129–3135.
- [15] S. Lohmeier, T. Buschmann, and H. Ulbrich, “Humanoid robot lola,” in *Robotics and Automation, 2009. ICRA '09. IEEE International Conference on*, 2009, pp. 775–780.
- [16] T. M. Corp. Partner robot family. [Online]. Available: http://www.toyota-global.com/innovation/partner_robot/family_2.html
- [17] I.-W. Park, J.-Y. Kim, and J.-H. Oh, “Online walking pattern generation and its application to a biped humanoid robot khr-3 (hubo),” *Advanced Robotics*, vol. 22, no. 2-3, pp. 159–190, 2008.
- [18] R. Tellez, F. Ferro, S. Garcia, E. Gomez, E. Jorge, D. Mora, D. Pinyol, J. Oliver, O. Torres, J. Velazquez, and D. Faconti, “Reem-b: An autonomous lightweight human-size humanoid robot,” in *Humanoid Robots, 2008. Humanoids 2008. 8th IEEE-RAS International Conference on*, 2008, pp. 462–468.
- [19] W. Kwon, H. Kim, J. K. Park, C. H. Roh, J. Lee, J. Park, W.-K. Kim, and K. Roh, “Biped humanoid robot mahru iii,” in *Humanoid Robots, 2007 7th IEEE-RAS International Conference on*, 2007, pp. 583–588.
- [20] M. Fujita, Y. Kuroki, T. Ishida, and T. Doi, “A small humanoid robot sdr-4x for entertainment applications,” in *Advanced Intelligent Mechatronics, 2003. AIM 2003. Proceedings. 2003 IEEE/ASME International Conference on*, vol. 2, 2003, pp. 938–943 vol.2.
- [21] M. Elmogy, C. Habel, and J. Zhang, “Online motion planning for hoap-2 humanoid robot navigation,” in *Intelligent Robots and Systems, 2009. IROS 2009. IEEE/RSJ International Conference on*, 2009, pp. 3531–3536.

- [22] D. Gouaillier, V. Hugel, P. Blazevic, C. Kilner, J. Monceaux, P. Lafortune, B. Marnier, J. Serre, and B. Maisonnier, “The nao humanoid: a combination of performance and affordability,” *CoRR*, pp. –1–1, July 2008.
- [23] I. Ha, Y. Tamura, H. Asama, J. Han, and D. Hong, “Development of open humanoid platform darwin-op,” in *SICE Annual Conference (SICE), 2011 Proceedings of*, 2011, pp. 2178–2181.
- [24] M. H. Raibert, “Legged robots that balance,” *Mathematical Biosciences*, vol. 85, no. 2, pp. 237 – 239, 1987. [Online]. Available: <http://www.sciencedirect.com/science/article/pii/0025556487900563>
- [25] J. Pratt, “Exploiting inherent robustness and natural dynamics in the control of bipedal walking robots,” Ph.D. dissertation, Computer Science Department, Massachusetts Institute of Technology, Cambridge, Massachusetts, 2000.
- [26] F. Moro, N. Tsagarakis, and D. Caldwell, “A human-like walking for the compliant humanoid coman based on com trajectory reconstruction from kinematic motion primitives,” in *Humanoid Robots (Humanoids), 2011 11th IEEE-RAS International Conference on*, 2011, pp. 364–370.
- [27] B. Lim, M. Lee, J. Kim, J. Lee, J. Park, K. Seo, and K. Roh, “Control design to achieve dynamic walking on a bipedal robot with compliance,” in *Robotics and Automation (ICRA), 2012 IEEE International Conference on*, 2012, pp. 79–84.
- [28] J. Pratt, J. Carff, S. Drakunov, and A. Goswami, “Capture point: A step toward humanoid push recovery,” in *Humanoid Robots, 2006 6th IEEE-RAS International Conference on*, 2006, pp. 200–207.
- [29] J. Pratt and B. Krupp, “Design of a bipedal walking robot,” vol. 6962. Spie, 2008, pp. 69 621F–69 621F–13. [Online]. Available: <http://link.aip.org/link/PSISDG/v6962/i1/p69621F/s1&Agg=doi>

- [30] C. Ott, C. Baumgartner, J. Mayr, M. Fuchs, R. Burger, D. Lee, O. Eiberger, A. Albu-Schaffer, M. Grebenstein, and G. Hirzinger, “Development of a biped robot with torque controlled joints,” in *Humanoid Robots (Humanoids), 2010 10th IEEE-RAS International Conference on*, 2010, pp. 167–173.
- [31] G. E. Lee, H. Bae, T. S. Yoon, J. S. Kim, T. I. Yi, and J. S. Park, “Factors that Influence Quiet Standing Balance of Patients with Incomplete Cervical Spinal Cord Injuries,” *Ann Rehabil Med*, vol. 36, no. 4, pp. 530–537, Aug 2012.
- [32] T. A. McMahon and P. R. Greene, “The influence of track compliance on running,” *Journal of Biomechanics*, vol. 12, no. 12, pp. 893 – 904, 1979. [Online]. Available: <http://www.sciencedirect.com/science/article/pii/0021929079900575>
- [33] Boston Dynamics. ATLAS The Agile Anthropomorphic Robot. [Online]. Available: <http://www.bostondynamics.com>
- [34] Y. Huang, Q. Wang, B. Chen, and L. Wang, “Effects of ankle stiffness on gait selection of dynamic bipedal walking with flat feet,” in *Rehabilitation Robotics (ICORR), 2011 IEEE International Conference on*, 2011, pp. 1–6.
- [35] D. T. Butterworth. Trajectory planning for 6 DOF manipulator using ROS and OMPL. [Online]. Available: <http://www.youtube.com/watch?v=IfP6J9Bxt2w>
- [36] A. H. Adiwahono, B. Liu, N. Chen, T. W. Chang, A. D. Tran, X. Wu, and B. S. Han, “System architecture for an interactive patrolling humanoid robot,” in *Proceedings of the Workshop at SIGGRAPH Asia*, ser. WASA '12. New York, NY, USA: ACM, 2012, pp. 119–123.
- [37] I.-W. Park, J.-Y. Kim, J. Lee, and J.-H. Oh, “Online free walking trajectory generation for biped humanoid robot khr-3(hubo),” in *Robotics and Automation, 2006. ICRA 2006. Proceedings 2006 IEEE International Conference on*, 2006, pp. 1231–1236.

- [38] F. Xue, X. Chen, J. Liu, and D. Nardi, “Real time biped walking gait pattern generator for a real robot,” in *RoboCup 2011: Robot Soccer World Cup XV*, ser. Lecture Notes in Computer Science, T. Rfer, N. Mayer, J. Savage, and U. Saranl, Eds. Springer Berlin Heidelberg, 2012, vol. 7416, pp. 210–221.
- [39] S. Hong, Y. Oh, Y.-H. Chang, and B.-J. You, “A walking pattern generation method for humanoid robots using least square method and quartic polynomial,” *Humanoid Robots*, 2009.
- [40] L. Righetti and A. Ijspeert, “Programmable central pattern generators: an application to biped locomotion control,” in *Robotics and Automation, 2006. ICRA 2006. Proceedings 2006 IEEE International Conference on*, 2006, pp. 1585–1590.
- [41] I.-W. Park and J.-Y. Kim, “Fourier series-based walking pattern generation for a biped humanoid robot,” in *Humanoid Robots (Humanoids), 2010 10th IEEE-RAS International Conference on*, 2010, pp. 461–467.
- [42] S. Kajita, F. Kanehiro, K. Kaneko, K. Fujiwara, K. Harada, K. Yokoi, and H. Hirukawa, “Biped walking pattern generation by using preview control of zero-moment point,” in *Robotics and Automation, 2003. Proceedings. ICRA '03. IEEE International Conference on*, vol. 2, 2003, pp. 1620–1626 vol.2.
- [43] O. Stasse, B. Verrelst, P.-B. Wieber, B. Vanderborght, P. Evrard, A. Kheddar, and K. Yokoi, “Modular architecture for humanoid walking pattern prototyping and experiments,” *Advanced Robotics, Special Issue on Middleware for Robotics –Software and Hardware Module in Robotics System*, vol. 22, no. 6, pp. 589–611, 2008.
- [44] O. Stasse, B. Verrelst, A. Davison, N. Mansard, F. Saidi, B. Vanderborght, C. Esteves, and K. Yokoi, “Integrating walking and vision to increase humanoid

- autonomy,” *International Journal of Humanoid Robotics, special issue on Cognitive Humanoid Robots*, vol. 5, no. 2, pp. 287–310, 2008.
- [45] P. B. Wieber, “Trajectory free linear model predictive control for stable walking in the presence of strong perturbations,” in *Humanoid Robots, 2006 6th IEEE-RAS International Conference on*, 2006, pp. 137–142.
- [46] C. Santacruz and Y. Nakamura, “Analytical real-time pattern generation for trajectory modification and footstep replanning of humanoid robots,” in *Intelligent Robots and Systems (IROS), 2012 IEEE/RSJ International Conference on*, 2012, pp. 2095–2100.
- [47] A. Thant and A. Khaing, “Application of cubic spline interpolation to walking patterns of biped robot,” *World Academy of Science Engineering and Technology*, vol. 50, p. 2734, 2009.
- [48] J.-W. Heo, I.-H. Lee, and J.-H. Oh, “Development of humanoid robots in hubo laboratory, kaist,” *Journal of the Robotics Society of Japan*, vol. 30, no. 4, pp. 367–371, 2012.
- [49] O. Stasse, A. Davison, R. Sellaouti, and K. Yokoi, “Real-time 3D SLAM for Humanoid Robot considering Pattern Generator Information,” in *IEEE/RSJ International Conference on Intelligent Robots and Systems*, October 2006, pp. 348–355.
- [50] K. Nishiwaki and S. Kagami, “High frequency walking pattern generation based on preview control of zmp,” in *Robotics and Automation, 2006. ICRA 2006. Proceedings 2006 IEEE International Conference on*, 2006, pp. 2667–2672.
- [51] B. Vanderborght, *Dynamic Stabilisation of the Biped Lucy Powered by Actuators with Controllable Stiffness*, ser. Springer Tracts in Advanced Robotics, B. Siciliano, O. Khatib, and F. Groen, Eds. Springer Tracts in Advanced Robotics, 2010, vol. 63, iISBN: 978-3-642-13416-6.

- [52] J. H. Strom, “Dynamically balanced omnidirectional humanoid robot locomotion,” Honors Thesis, Bowdoin College, 2009.
- [53] D. Gouaillier, C. Collette, and C. Kilner, “Omni-directional closed-loop walk for nao,” in *Humanoid Robots (Humanoids), 2010 10th IEEE-RAS International Conference on*, 2010, pp. 448–454.
- [54] Y. Jun, R. Ellenberg, and P. Oh, “Realization of miniature humanoid for obstacle avoidance with real-time zmp preview control used for full-sized humanoid,” in *Humanoid Robots (Humanoids), 2010 10th IEEE-RAS International Conference on*, 2010, pp. 46–51.
- [55] S. Kajita, K. Harada, F. Kanehiro, K. Kaneko, K. Fujiwara, K. Yokoi, , and H. Hirukawa, “A dynamics filter for zmp compensation by preview control (in japanese),” in *In Proceedings of the 21st Annual Conference of the Robotics Society in Japan*, 2003, p. page 3A18.
- [56] S. Kajita, *Humanoid Robot*. Japan: Ohmsha (in Japanese), 2005, iISBN 4-274-20058-2.
- [57] J. Park and Y. Youm, “General zmp preview control for bipedal walking,” in *Robotics and Automation, 2007 IEEE International Conference on*, 2007, pp. 2682–2687.
- [58] A. Herdt, D. Holger, P. Wieber, D. Dimitrov, K. Mombaur, and D. Moritz, “Online walking motion generation with automatic foot step placement,” *Advanced Robotics*, vol. 24, pp. 719–737, 2010.
- [59] D. Dimitrov, P. B. Wieber, H. J. Ferreau, and M. Diehl, “On the implementation of model predictive control for on-line walking pattern generation,” in *Proceedings of the IEEE International Conference on Robotics and Automation (ICRA)*, 2008, pp. 2685–2690.

- [60] H. Diedam, D. Dimitrov, P. B. Wieber, K. Mombaur, and M. Diehl, “Online walking gait generation with adaptive foot positioning through linear model predictive control,” in *Intelligent Robots and Systems, 2008. IROS 2008. IEEE/RSJ International Conference on*, 2008, pp. 1121–1126.
- [61] ODE (Open Dynamics Engine) , “Open-source simulator for rigid body dynamics.” [Online]. Available: <http://www.ode.org>
- [62] Bullet Physics Engine, “Open-source physics library.” [Online]. Available: <http://www.bulletphysics.org>
- [63] Critical Mass Labs, “Vortex physics toolkit.” [Online]. Available: <http://www.vxsim.com>
- [64] Gazebo, “Open-source robotics simulator.” [Online]. Available: <http://www.gazebosim.org>
- [65] OpenRAVE, “Open robotics automation virtual environment.” [Online]. Available: <http://www.openrave.org>
- [66] V-REP, “Robot simulator.” [Online]. Available: <http://www.coppeliarobotics.com>
- [67] O. Michel, “Webots: Professional Mobile Robot Simulation,” *Journal of Advanced Robotics Systems*, vol. 1, no. 1, pp. 39–42, 2004.
- [68] MORSE, “Modular OpenRobots Simulation Engine.” [Online]. Available: <http://www.openrobots.org/wiki/morse>
- [69] OpenHRP, “Open Architecture Humanoid Robotics Platform.” [Online]. Available: <http://www.openrtp.jp/openhrp3/en>
- [70] H. Hirukawa, F. Kanehiro, S. Kajita, K. Fujiwara, K. Yokoi, K. Kaneko, and K. Harada, “Experimental evaluation of the dynamic simulation of biped walk-

- ing of humanoid robots,” in *Robotics and Automation, 2003. Proceedings. ICRA '03. IEEE International Conference on*, vol. 2, 2003, pp. 1640–1645.
- [71] P. Cominoli, “Development of a physical simulation of a real humanoid robot,” Ph.D. dissertation, EPFL, Swiss Federal Institute of Technology, 2005.